

Low-complexity method for hybrid MPC with local optimality guarantees [★]

Damian Frick ^a, Juan L. Jerez ^{a,b}, Alexander Domahidi ^{b,c}, Angelos Georghiou ^d,
Manfred Morari ^a

^a*Automatic Control Laboratory, ETH Zürich, Physikstrasse 3, 8092 Zürich, Switzerland*

^b*embotech GmbH, Physikstrasse 3, 8092 Zürich, Switzerland*

^c*inspire AG, Technoparkstrasse 1, 8005 Zürich, Switzerland*

^d*Desautels Faculty of Management, McGill University, Montreal, Quebec, Canada*

Abstract

Model predictive control problems for constrained hybrid systems are usually cast as mixed-integer optimization problems (MIP). However, commercial MIP solvers are designed to run on desktop computing platforms and are not suited for embedded applications which are typically restricted by limited computational power and memory. To alleviate these restrictions, we develop a novel low-complexity, iterative method for a class of non-convex, non-smooth optimization problems. This class of problems encompasses hybrid model predictive control problems where the dynamics are piece-wise affine (PWA). We give conditions under which the proposed algorithm has fixed points and show that, under practical assumptions, our method is guaranteed to converge locally to local minima. This is in contrast to other low-complexity methods in the literature, such as the non-convex alternating directions method of multipliers (ADMM), that give no such guarantees for this class of problems. By interpreting the PWA dynamics as a union of polyhedra we can exploit the problem structure and develop an algorithm based on operator splitting procedures. Our algorithm departs from the traditional MIP formulation, and leads to a simple, embeddable method that only requires matrix-vector multiplications and small-scale projections onto polyhedra. We illustrate the efficacy of the method on a numerical example, achieving performance close to the global optimum with computational times several orders of magnitude smaller compared to state-of-the-art MIP solvers. Moreover, it is competitive with ADMM in terms of suboptimality and computation time, but additionally provides local optimality and local convergence guarantees.

Key words: Operator splitting; Hybrid model predictive control; Non-smooth and discontinuous problems; Iterative schemes.

1 Introduction

Many practical applications for control fall in the domain of hybrid systems, including applications such as active suspension control or energy management in automobiles [1,2] and applications in power electronics [3].

These applications require fast sampling times in the sub-second range, and the control algorithms need to be implemented on industrial, resource-constrained platforms, such as microcontrollers or re-configurable hardware. These systems are characterized by complex interactions between discrete and continuous behaviors that make them extremely challenging to control. In the last decades model predictive control (MPC) [4] has received widespread attention both in research and industry. This technique provides a systematic approach for controlling constrained hybrid systems, promising high control performance with minimal tuning effort.

For hybrid systems, mature modeling tools such as the mixed logical dynamical framework, see [5], are available. It defines rules for posing hybrid MPC as mixed-integer optimization problems (MIP). These MIPs can then be tackled with powerful commercial solvers such

[★] This manuscript is the preprint of a paper submitted to *Automatica* and is subject to Elsevier copyright. Elsevier maintains the sole rights of distribution or publication of the work in all forms and media. If accepted, the copy of record will be available at <http://www.journals.elsevier.com/automatica/>.

Email addresses: dafrick@control.ee.ethz.ch (Damian Frick), juanlj@control.ee.ethz.ch (Juan L. Jerez), domahidi@inspire.ethz.ch (Alexander Domahidi), angelos.georghiou@mcgill.ca (Angelos Georghiou), morari@control.ee.ethz.ch (Manfred Morari).

as CPLEX [6]. These solvers have focused on the solution of generic, large-scale, mixed-integer linear and quadratic programming problems on powerful computing platforms. This has several drawbacks for embedded applications: (i) their code size is in the order of tens of megabytes; (ii) the algorithms require substantial working memory; (iii) they depend on numerical libraries that cannot be ported to most embedded platforms. This has restricted the applicability of hybrid MPC to systems that can run on desktop computing platforms, with sampling times in the order of minutes or even hours.

Recently there have been efforts to enable hybrid MPC applications with faster dynamics to run on platforms with more limited computational power. Explicit MPC [7] is the method of choice for very small problems but quickly becomes intractable. Therefore, methods that further exploit (i) the sparsity-inducing multistage structure of MPC problems, and (ii) the fact that MPC problems are parametric and solved in a receding horizon fashion, have been developed. Methods based on MIP reformulations have been investigated, see [8–11], and have led to reduced computation times compared to general-purpose solvers. However, these methods are not fast enough for many practical applications.

Methods based on operator splitting allow to trade off computational complexity with optimality, i.e., they typically produce “good” solutions in a fraction of the time required even by tailored MIP solvers to find global optima. Furthermore, they allow the problem to be split into several small subproblems, making these methods especially suited for embedded applications and implementations on computing systems with highly limited resources. The alternating directions method of multipliers (ADMM) [12] is an example of such operator splitting methods. In [13], ADMM was used on various hybrid MPC examples achieving substantial gains in computational performance compared to general-purpose MIP solvers. Convergence guarantees are available for some special cases of non-convex ADMM [14, 15], however, neither optimality or convergence guarantees are available for the case of hybrid MPC. Other low-complexity methods based on operator splitting suited for non-convex MPC are [16, 17]. They are attractive because they offer computational performance similar to ADMM, but unlike ADMM they still retain some guarantees on optimality and convergence. Nonetheless, they do not address the class of hybrid MPC problems considered here.

1.1 Contribution

In this paper, we develop an algorithm based on operator splitting to address hybrid MPC problems, that provides both the desired theoretical guarantees, and computational speed. Our method exploits the multistage structure of the optimization problem, allowing to decompose the complex piece-wise affine (PWA) equality constraints into decoupled non-convex polyhedral constraints. By leveraging their polyhedral nature, we are

able to derive guarantees on optimality and convergence. The main contributions of this paper are the following:

- We develop an iterative, numerical method to find local minima of a class of non-convex, non-smooth optimization problems that arise in MPC problems for systems with PWA dynamics. Our method is of low complexity and only requires matrix-vector multiplications and small-scale Euclidean projections onto convex polyhedra.
- We provide (i) conditions for the existence of fixed points of the proposed algorithm; (ii) show that the method converges locally to such fixed points; and (iii) prove that fixed points correspond to local minima. To the author’s knowledge, for the class of problems considered, this is the first method of such simplicity that allows to give local optimality and convergence guarantees.
- The proposed algorithm is implemented using automatic code generation, directly targeting the embedded applications. This code generation tool is made publicly available via github [18]. We examine the method’s performance on a numerical example and demonstrate computational speed-ups of several orders of magnitude, compared to conventional MIP solvers, with only a minor loss of optimality. We further show, that the method is competitive with other local methods such as ADMM.

1.2 Outline

In Section 2, we state the problem. In Section 3, we construct an operator whose fixed points correspond to local minima. In Section 4, we propose an algorithm based on this operator and discuss local optimality and local convergence of the method. In Section 5, we present numerical results. Proofs of auxiliary results are given in Appendix C.

1.3 Notation & elementary definitions

For vectors $x, y \in \mathbb{R}^n$, $\|x\| := \sqrt{x^\top x}$ is the 2-norm and $\langle x, y \rangle := x^\top y$ the scalar product. For a closed set \mathcal{C} , $\mathcal{P}_{\mathcal{C}}(x) := \arg \min_{z \in \mathcal{C}} \|x - z\|$ is the Euclidean projection of x onto \mathcal{C} . The closed ϵ -ball around x is $\mathcal{B}_\epsilon(x) := \{z \mid \|x - z\| \leq \epsilon\}$, we use the shorthand $\mathcal{B}_\epsilon := \mathcal{B}_\epsilon(0)$. The *relative interior* is $\text{relint } \mathcal{C}$. By $\mathcal{C} + \{x\}$ we denote the Minkowski sum of \mathcal{C} and the singleton x . The *characteristic function* of set \mathcal{C} is $\chi_{\mathcal{C}}(x) := \{0 \text{ if } x \in \mathcal{C}; +\infty \text{ otherwise}\}$. An *operator* $T : \mathcal{X} \rightrightarrows \mathcal{Y}$ maps every point $x \in \mathcal{X}$ to a set $T(x) \subseteq \mathcal{Y}$. T is called *single-valued* if for all $x \in \mathcal{X}$: $T(x)$ is a singleton. A *zero* of T is a point $x \in \mathcal{X}$ such that $0 \in T(x)$, denoted by $x \in \text{zero } T$, where $\text{zero } T := \{x \mid 0 \in T(x)\}$. A *fixed point* of T is a point $x \in \mathcal{X}$ such that $x \in T(x)$, denoted by $x \in \text{fix } T$, where $\text{fix } T := \{x \mid x \in T(x)\}$.

2 Problem statement

In this work, we consider optimization problems that are *parametric* in $\theta \in \mathbb{R}^p$ and given as follows:

$$p^*(\theta) := \min_{z \in \mathcal{E} \cap \mathcal{Z}(\theta)} \frac{1}{2} z^\top H z + h^\top z, \quad (1a)$$

with $H \in \mathbb{R}^{n \times n}$ positive definite, and $z := (z_1, \dots, z_N) \in \mathbb{R}^n$, with $z_k \in \mathbb{R}^{n_k}$. The parametric nature implies that only parts of the problem data will change every time the solved is invoked. The non-convex set $\mathcal{Z}(\theta) \subseteq \mathbb{R}^n$ is:

$$\mathcal{Z}(\theta) := \bigtimes_{k=1}^N \left(\bigcup_{i=1}^{m_k} \mathcal{Z}_{k,i}(\theta) \right), \quad (1b)$$

and the sets $\mathcal{Z}_{k,i}(\theta) \subseteq \mathbb{R}^{n_k}$ are closed convex polyhedra that may depend linearly on θ , in the following way:

$$\mathcal{Z}_{k,i}(\theta) := \{z_k \in \mathbb{R}^{n_k} \mid F_{k,i} z_k \leq f_{k,i}(\theta), \\ G_{k,i} z_k = g_{k,i}(\theta)\},$$

with matrices and vectors of appropriate dimensions, and $f_{k,i}(\theta)$, $g_{k,i}(\theta)$ affine functions of the parameter θ . For a given parameter θ , the Euclidean projection onto $\mathcal{Z}(\theta)$ can be evaluated very efficiently by decoupling it into simple convex projections, see Algorithm 2 in Section 4. This important feature of \mathcal{Z} will be a key ingredient of the algorithm presented in Section 4. For simplicity of notation we will omit the parameter dependence of $\mathcal{Z}(\theta)$ in the remainder of this paper. Finally, the set \mathcal{E} is an affine equality constrained set $\mathcal{E} := \{z \in \mathbb{R}^n \mid Az = b\} = \{Vv + \bar{v} \mid v \in \mathbb{R}^{n-m}\}$, with $A \in \mathbb{R}^{m \times n}$ full row rank, and an appropriate matrix $V \in \mathbb{R}^{n \times n-m}$ and vector $\bar{v} \in \mathbb{R}^m$ [19, p. 430, (15.14)], where V has full column rank by construction. We furthermore assume that $\mathcal{E} \cap \mathcal{Z}$ is non-empty, hence the problem is feasible.

2.1 Consensus form

Problem (1) can be re-written in the so-called consensus form by introducing copies y of z as follows

$$p^* := \min_{z, y : z=y} \frac{1}{2} z^\top H z + h^\top z + \chi_{\mathcal{E}}(z) + \chi_{\mathcal{Z}}(y), \quad (2)$$

which is a non-convex, non-smooth optimization problem. The constraint sets \mathcal{E} and \mathcal{Z} have been moved into the cost function using their characteristic functions $\chi_{\mathcal{E}}(z)$ and $\chi_{\mathcal{Z}}(y)$. This problem formulation ensures that the two sets \mathcal{E} and \mathcal{Z} can be decoupled. The consensus constraint $z = y$ encodes the coupling between z and y .

2.2 Model Predictive Control

We are particularly interested in MPC problems where the discrete dynamics are given by a PWA function of the

states and inputs. Such parametric hybrid MPC problems can be written as:

$$\min_{x_k, u_k} \sum_{k=1}^N q_{k+1}(x_{k+1}) + r_k(u_k) \quad (3a)$$

$$\text{s. t. } x_{k+1} = A_{k,i} x_k + B_{k,i} u_k + c_{k,i}, \\ \text{if } (x_k, u_k) \in \mathcal{C}_{k,i}, k = 1, \dots, N, \quad (3b)$$

$$x_1 = \theta, \quad (3c)$$

for $i = 1, \dots, m_k$ with m_k representing the number of regions of the PWA dynamics. Vector $x_k \in \mathbb{R}^{n_x}$ denotes the state of the system at time k , $u_k \in \mathbb{R}^{n_u}$ denotes the inputs applied to the system between times k and $k+1$, and $\theta \in \mathbb{R}^{n_x}$ is the (parametric) initial state of the system. The objective terms q_{k+1} and r_k are strictly convex, quadratic functions. The sets $\mathcal{C}_{k,i}$ are non-empty, closed, convex polyhedra that define the partition of the PWA dynamics, and include state and input constraints.

Problems of the form (3) can be solved by introducing additional continuous and binary variables, and formulating an MIP using, e.g., the big-M reformulation [5] or more advanced formulations [20]. The resulting programs can be solved using powerful, commercial MIP solvers. Instead of formulating a MIP, in this work we transform Problem (3) into the form (1). In this way only Nn_x auxiliary continuous variables and *no binary variables* need to be introduced. For each time instant k we introduce a copy w_k of x_{k+1} , as follows:

$$w_k := A_{k,i} x_k + B_{k,i} u_k + c_{k,i}, \text{ for } (x_k, u_k) \in \mathcal{C}_{k,i}. \quad (4a)$$

This allows us to define the convex, polyhedral sets

$$\mathcal{Z}_{1,\hat{i}}(\theta) := \{(u_1, w_1) \mid w_1 = A_{1,\hat{i}} \theta + B_{1,\hat{i}} u_1 + c_{1,\hat{i}}, \\ \text{and } (\theta, u_1) \in \mathcal{C}_{1,\hat{i}}\}, \\ \mathcal{Z}_{k,i} := \{(x_k, u_k, w_k) \mid \text{such that (4a) holds}\},$$

for $\hat{i} = 1, \dots, m_1$ and for $i = 1, \dots, m_k$, $k = 2, \dots, N$. The sets $\mathcal{Z}_{k,i}$ are closed by construction. The non-convex constraint set \mathcal{Z} now has the form of (1b) and is *decoupled* in the horizon N . For an equivalent formulation, we impose $x_{k+1} = w_k$ by defining a set of *coupling* equality constraints

$$\mathcal{E} := \bigtimes_{k=1}^N \left(\mathbb{R}^{n_u} \times \{(w_k, x_{k+1}) \in \mathbb{R}^{2n_x} \mid x_{k+1} = w_k\} \right).$$

Remark 1 To ensure the strict convexity of Problem (1) equivalent to Problem (3), we impose the objective:

$$\alpha_k q_{k+1}(x_{k+1}) + (1 - \alpha_k) q_{k+1}(w_k),$$

for each k and any $\alpha_k \in (0, 1)$. With the coupling constraint $w_k = x_{k+1}$ this ensures that the cost remains unchanged. In this work, we have used $\alpha_k = 0.5$ for all k .

3 KKT conditions for Problem (2)

We investigate Karush-Kuhn-Tucker (KKT) conditions for Problem (2) and construct an operator K_ξ for finding particular KKT points. The properties and structure of this operator play an important role in showing local optimality and local convergence properties as well as establishing the computational efficiency of the method.

3.1 Generalized, regular & proximal KKT points

In the context of convex optimization the KKT conditions give rise to necessary and sufficient conditions for global optimality. In the non-convex, non-smooth case, however, they are in general neither necessary nor sufficient, even for local optimality. We use a notion of KKT points for instances of Problem (2) that give rise to necessary conditions for local optimality. Computing such KKT points is in general intractable. Therefore, we propose two inner approximations that are more computationally attractive. We denote KKT points by \dagger , local optima by \circ and global optima by $*$.

A point $(z^\dagger, y^\dagger, \lambda^\dagger)$ is called a (generalized) KKT point [21, Theorem 3.34, p. 127] of Problem (2) if it satisfies

$$0 \in \{Hz^\dagger + h\} + \mathcal{N}_\mathcal{E}(z^\dagger) - \{\lambda^\dagger\}, \quad (5a)$$

$$0 \in \mathcal{N}_\mathcal{Z}(y^\dagger) + \{\lambda^\dagger\}, \quad (5b)$$

$$0 = z^\dagger - y^\dagger, \quad (5c)$$

where the regular normal cone of a set \mathcal{C} is denoted by

$$\hat{\mathcal{N}}_\mathcal{C}(z) := \left\{ x \in \mathbb{R}^n \mid \limsup_{u \rightarrow z} \frac{\langle x, u - z \rangle}{\|u - z\|} \right\}, \text{ and}$$

$$\mathcal{N}_\mathcal{C}(z) := \limsup_{x \rightarrow z} \hat{\mathcal{N}}_\mathcal{C}(x) = \partial\chi_\mathcal{C}(z),$$

denotes the (limiting) normal cone as defined in [22, Proposition 6.5, p. 200]. In particular, (5) implies that $z^\dagger = y^\dagger \in \mathcal{E} \cap \mathcal{Z}$. Since any KKT point $(z^\dagger, y^\dagger, \lambda^\dagger)$ satisfies primal feasibility, $z^\dagger = y^\dagger$, we will use the shorthand notation $(z^\dagger, \lambda^\dagger)$ for KKT points in the remainder of this paper. The KKT conditions (5) give rise to necessary conditions for local optimality as detailed below.

Lemma 1 (Necessary optimality condition) *For every local minimum z° of Problem (2) there exist Lagrange multipliers $\lambda^\circ \in \mathbb{R}^n$ such that (z°, λ°) is a (generalized) KKT point of Problem (2).*

These KKT conditions are difficult to use due to the dependence on the normal cone of \mathcal{Z} , which cannot be evaluated easily [23]. However, we can define two inner approximations that admit practical characterizations, resulting in what we call *regular* and *ξ -proximal* KKT points. These special cases of KKT points can be evaluated more efficiently and have important regularity properties. Furthermore, in Section 4.2, we will show

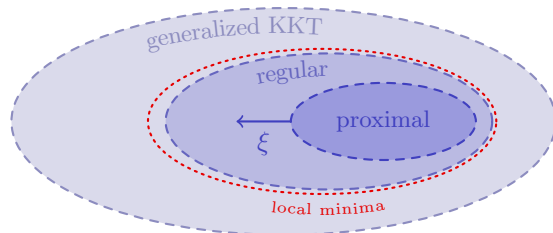


Fig. 1. Conceptual illustration of the relationship between generalized, regular and proximal KKT points (dashed). The sets represent points z for which there exist multipliers λ such that (z, λ) is a generalized, regular or proximal KKT point, as well as the set of local minima (dotted).

that they provide sufficient (but no longer necessary) conditions for local optimality.

We call a point $(z^\dagger, \lambda^\dagger)$ a *regular* KKT point of Problem (2), if it satisfies

$$0 \in \{Hz^\dagger + h\} + \hat{\mathcal{N}}_\mathcal{E}(z^\dagger) - \{\lambda^\dagger\}, \text{ and} \quad (6a)$$

$$0 \in \hat{\mathcal{N}}_\mathcal{Z}(z^\dagger) + \{\lambda^\dagger\}. \quad (6b)$$

Note that we have replaced the normal cone $\mathcal{N}_\mathcal{Z}(z^\dagger)$ from (5b) with the regular normal cone $\hat{\mathcal{N}}_\mathcal{Z}(z^\dagger)$. Since $\hat{\mathcal{N}}_\mathcal{Z}(z^\dagger) \subseteq \mathcal{N}_\mathcal{Z}(z^\dagger)$, according to [22, Proposition 6.5, p. 200], the set of regular KKT points is an inner approximation of the set of (generalized) KKT points.

Given $\xi > 0$, we call a point $(z^\dagger, \lambda^\dagger)$ a *ξ -proximal* KKT point of Problem (2), if it satisfies

$$0 \in \{Hz^\dagger + h\} + \hat{\mathcal{N}}_\mathcal{E}(z^\dagger) - \{\lambda^\dagger\}, \text{ and} \quad (7a)$$

$$z^\dagger \in \mathcal{P}_\mathcal{Z}(z^\dagger - \frac{1}{\xi}\lambda^\dagger). \quad (7b)$$

Compared to the definition of regular KKT points we have replaced (6b) with a condition on the projection, and we have introduced a positive scaling ξ using $z^\dagger \in \mathcal{P}_\mathcal{Z}(z^\dagger - \frac{1}{\xi}\lambda^\dagger) \Rightarrow -\frac{1}{\xi}\lambda^\dagger \in \hat{\mathcal{N}}_\mathcal{Z}(z^\dagger)$, which follows from [22, Example 6.16, p. 212]. This directly implies that every ξ -proximal KKT point $(z^\dagger, \lambda^\dagger)$ is also a regular KKT point and therefore (7) is an inner approximation of (6).

Evaluating whether a pair (z, λ) is a regular KKT point has an exponential worst-case complexity, because representing $\hat{\mathcal{N}}_\mathcal{Z}(z)$ may be combinatorial and can quickly become intractable. In contrast, evaluating whether a pair (z, λ) is a ξ -proximal KKT point amounts to a projection that can be performed in polynomial-time. Furthermore, for the primal variables z , this inner approximation (7) of (6) can be made tight. This is seen via the following proposition which relates any regular KKT point to a ξ -proximal KKT point. Figure 1 illustrates the conceptual relationship between the different KKT points.

Proposition 1 *Consider Problem (2). Then*

- i) for any regular KKT point $(z^\dagger, \lambda^\dagger)$, there exists a $\bar{\xi} > 0$ s.t. for all $\xi \geq \bar{\xi}$, $(z^\dagger, \lambda^\dagger)$ is a ξ -proximal KKT point.
ii) Given any $\xi > 0$ and ξ -proximal KKT point $(z^\dagger, \lambda^\dagger)$, then $(z^\dagger, \lambda^\dagger)$ is also a regular KKT point.

Problem (2) has only finitely many local minima due to positive definiteness of H and the polyhedrality of $\mathcal{E} \cap \mathcal{Z}$. Therefore, given a $\xi > 0$ large enough, for every regular KKT point $(z^\dagger, \lambda^\dagger)$ there exists a μ^\dagger such that (z^\dagger, μ^\dagger) is a ξ -proximal KKT point.

3.2 Operator for proximal KKT points

The polynomial-time set-membership evaluation of (7) motivates the construction of an operator K_ξ that has the property that (i) it is cheap to evaluate and (ii) has zeros corresponding to ξ -proximal KKT points of Problem (2). We define a set-valued operator $K_\xi : \mathbb{R}^n \rightrightarrows \mathbb{R}^n$:

$$K_\xi(s) := \{M_\xi s + c_\xi\} - \mathcal{P}_{\mathcal{Z}}(s), \quad (8a)$$

with $\xi > 0$ the proximal scaling, and

$$M_\xi := \xi(\xi R - I)^{-1} R, \quad (8b)$$

$$c_\xi := (\xi R - I)^{-1} (R(h + H\bar{v}) - \bar{v}), \quad (8c)$$

$$R := V(V^\top H V)^{-1} V^\top, \quad (8d)$$

where V and \bar{v} are as defined in Section 2. Finding an s such that $0 \in K_\xi(s)$ is equivalent to finding a pair (z, λ) that satisfies the ξ -proximal KKT conditions in (7).

For K_ξ to be defined properly, we need invertibility of $\xi R - I$. Since $R \succeq 0$, it follows that this holds for all

$$\xi > (\lambda_{\min}^+(R))^{-1}. \quad (9a)$$

$$\text{This implies } M_\xi \succeq 0 \text{ and } \lambda_{\min}^+(M_\xi) > 1, \quad (9b)$$

where $\lambda_{\min}^+(R)$ is the smallest non-zero eigenvalue of R . For Problem (3), it can be shown that $\xi > \lambda_{\max}(H)$ is necessary and sufficient for satisfying both (9a) and (9b). To achieve the theoretical guarantees in Section 4, we will need to impose further lower bounds on ξ .

Using (8a) we can show that points $s^\dagger \in \text{zero } K_\xi$, correspond to ξ -proximal KKT points $(z^\dagger, \lambda^\dagger)$ as follows:

$$z^\dagger := M_\xi s^\dagger + c_\xi \text{ and } \lambda^\dagger := \xi(z^\dagger - s^\dagger), \quad (10)$$

where the precise relationship is presented in Lemma 2.

Lemma 2 (Zeros of operator K_ξ) *Given any $\xi > 0$, a point s^\dagger is a zero of K_ξ , i.e., $s^\dagger \in \text{zero } K_\xi$ if and only if the pair $(z^\dagger, \lambda^\dagger)$ constructed through (10) is a ξ -proximal KKT point of Problem (2).*

M_ξ is only invertible when $\mathcal{E} = \mathbb{R}^n$, thus multiple vectors $s^\dagger \in \text{zero } K_\xi$ can result in the same z^\dagger (but different λ^\dagger).

4 Solution method and theoretical guarantees

We now present a method for finding ξ -proximal KKT points of Problem (2) by finding zeros of the operator K_ξ . The basis of this method is a fixed-point iteration. We have argued that K_ξ can be evaluated efficiently because it only involves matrix-vector multiplications and a small number of projections onto convex polyhedra. Therefore every iteration computationally inexpensive. In addition, we will show that every zero of K_ξ corresponds to a local minimum of Problem (2). Finally, we will show that, under some assumptions, our algorithm converges locally to such minima, almost always. By ‘almost always’ we mean that, for any local minimum that has corresponding fixed points, there exist at most a measure-zero subset of fixed points from which the method may not converge.

4.1 Fixed-point algorithm

We define an operator $T_\xi : \mathbb{R}^n \rightrightarrows \mathbb{R}^n$, that has the zeros of K_ξ as its fixed points:

$$\begin{aligned} T_\xi(s) &:= s - W K_\xi(s) \\ &= s - W(M_\xi s + c_\xi - \mathcal{P}_{\mathcal{Z}}(s)) \end{aligned} \quad (11a)$$

The invertible weighting matrix W , chosen as

$$W := Q \begin{pmatrix} \frac{1}{2}\Lambda^{-1} & 0 \\ 0 & -I \end{pmatrix} Q^\top, \quad (11b)$$

where $Q \in \mathbb{R}^{n \times n}$ is orthonormal and $\Lambda \in \mathbb{R}^{n-m \times n-m}$ diagonal, positive definite, such that $M_\xi = Q \text{diag}(\Lambda, 0) Q^\top$ is the eigendecomposition of M_ξ . The invertibility of W ensures that $\text{fix } T_\xi = \text{zero } K_\xi$. In addition, the structure of W will be used to prove local non-expansiveness of the operator T_ξ , see Lemma 5 in Section 4.4.

Algorithm 1 Solution method for Problem (2)

Require: $s_0 \in \mathbb{R}^n$, $\gamma \in (0, 1)$, $\epsilon_{\text{tol}} > 0$
1: **if** $z^* := \bar{v} - R(h + H\bar{v}) \in \mathcal{Z}$ **then return** z^*
2: **repeat from** $j = 0$
3: $z_{j+1} = M_\xi s_j + c_\xi$
4: $y_{j+1} \in \mathcal{P}_{\mathcal{Z}}(s_j)$ ▷ Projection, see Alg. 2
5: $s_{j+1} = s_j - \gamma W(z_{j+1} - y_{j+1})$
6: $j \leftarrow j + 1$
7: **until** $\|z_j - y_j\| \leq \epsilon_{\text{tol}}$
8: **return** y_j

The local non-expansiveness of T_ξ allows us to use the *Krasnoselskij iteration* [24, Theorem 3.2, p. 65] to find fixed points of T_ξ . Given an initial iterate s_0 , the Krasnoselskij iteration is defined as follows:

$$s_{j+1} = (1 - \gamma)s_j + \gamma T_\xi(s_j), \quad (11c)$$

with step size $\gamma \in (0, 1)$.

From (11c) we obtain Algorithm 1. Each iteration of Algorithm 1 is simple and geared towards an efficient embedded implementation utilizing automatic code-generation. The most expensive step is the projection onto the non-convex set \mathcal{Z} in step 4. For problems of the form (3), the matrices M_ξ and W are block-banded with bandwidth $\max\{2n_x, n_u\}$, therefore steps 3 and 5 of Algorithm 1 can be evaluated very efficiently and have a computational complexity of $\mathcal{O}(N(n_x + n_u)^2)$. The projection in step 4 can be evaluated in polynomial time using Algorithm 2, where at most $\sum_{k=1}^N m_k$ small-scale projections $\mathcal{P}_{\mathcal{Z}_{k,i}(\theta)}(s_k)$ onto polyhedra need to be computed (step 3, Algorithm 2). State-of-the-art embedded solvers [25] or even explicit solutions [26] can be used for these projections. This enables the automatic generation of efficient, embeddable code that is tailored to particular (parametric) problems.

Algorithm 2 $\mathcal{P}_{\mathcal{Z}}(s)$, projection of s onto \mathcal{Z}

Require: $s = (s_1, \dots, s_N) \in \mathbb{R}^n$, \mathcal{Z} of form (1b)

- 1: **for** $k = 1, \dots, N$ **do**
- 2: **for** $i = 1, \dots, m_k$ **do**
- 3: $z_{k,i} = \mathcal{P}_{\mathcal{Z}_{k,i}}(s_k)$ \triangleright simple
- 4: $z_k \in \arg \min_{i=1, \dots, m_k} \|s_k - z_{k,i}\|$
- 5: **return** $z = (z_1, \dots, z_N)$

It should be noted that while the simplicity of Algorithm 1 is reminiscent of ADMM, the algorithms have important differences that make it possible to give local optimality and convergence guarantees in our case.

4.2 Local optimality

Firstly, we will show that for Problem (2) any regular KKT point corresponds to a local minimum. This immediately implies that the fixed points of the operator T_ξ also correspond to local minima. Using distributivity of the Cartesian product over unions, we can transform the representation (1b) of \mathcal{Z} into a representation as the finite union of closed, convex polyhedra $\mathcal{Z}^i \subseteq \mathbb{R}^n$ with $\mathcal{Z} = \bigcup_{i=1}^I \mathcal{Z}^i$, where $I := \prod_{k=1}^N m_k$. A set of form (1b) always admits such a representation which helps to simplify our theoretical considerations. The finite union representation is not suited for computational purposes and the exact construction of the sets \mathcal{Z}^i does not affect the presented results. Furthermore, we define the set of active components of \mathcal{Z} at a point $z \in \mathcal{Z}$ as $\mathcal{I}_{\mathcal{Z}}(z) := \{i \in \{1, \dots, I\} \mid z \in \mathcal{Z}^i\}$.

To establish the subsequent theoretical results we will use the polar $\hat{\mathcal{N}}_{\mathcal{Z}}^*$ of the regular normal cone, defined in [22, Equation 6(14), p. 215] as

$$\hat{\mathcal{N}}_{\mathcal{Z}}^*(z) = \{v \mid \langle v, w \rangle \leq 0, \forall w \in \hat{\mathcal{N}}_{\mathcal{Z}}(z)\}.$$

The following lemma establishes two important proper-

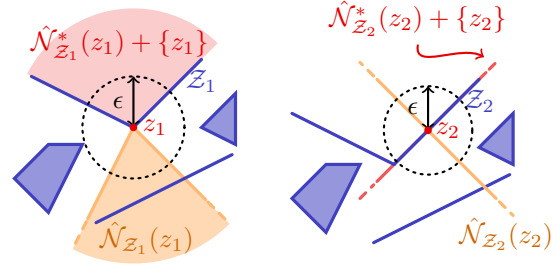


Fig. 2. Two cases of local convexifications $\hat{\mathcal{N}}_{\mathcal{Z}}^*(z) + \{z\}$ of non-convex sets \mathcal{Z}_1 and \mathcal{Z}_2 at points z_1 (left) and z_2 (right), as described in Lemma 3.

ties of the set \mathcal{Z} and its normal cone. These properties will be used in Theorem 1 for proving local optimality. At any point $z \in \mathcal{Z}$, Lemma 3 relates the set \mathcal{Z} to a local convexification $\hat{\mathcal{N}}_{\mathcal{Z}}^*(z) + \{z\}$, as illustrated in Figure 2.

Lemma 3 For any $z \in \mathcal{Z}$, the set \mathcal{Z} and the closed convex set $\hat{\mathcal{N}}_{\mathcal{Z}}^*(z) + \{z\}$ are related in the following ways:

- i) There exists an $\bar{\epsilon} > 0$ such that for all $\epsilon \in (0, \bar{\epsilon}]$ it holds that $\mathcal{Z} \cap \mathcal{B}_\epsilon(z) \subseteq \hat{\mathcal{N}}_{\mathcal{Z}}^*(z) + \{z\}$.
- ii) Their regular normal cones evaluated at z coincide, i.e., $\hat{\mathcal{N}}_{\mathcal{Z}}(z) = \hat{\mathcal{N}}_{\hat{\mathcal{N}}_{\mathcal{Z}}^*(z) + \{z\}}(z)$.

We now use Lemma 3 to prove the first key result.

Theorem 1 (Sufficient local optimality condition)

If $(z^\dagger, \lambda^\dagger)$ is a regular KKT point of Problem (2), then z^\dagger is a local minimum of Problem (2).

PROOF. Let $(z^\dagger, \lambda^\dagger)$ be a regular KKT point of Problem (2). We consider the auxiliary problem:

$$\min_{z, y: z=y} \frac{1}{2} z^\top H z + h^\top z + \chi_{\mathcal{E} \times (\hat{\mathcal{N}}_{\mathcal{Z}}^*(z^\dagger) + \{z^\dagger\})}(z, y). \quad (13)$$

Problem (13) is strictly convex and its KKT conditions are given as $z = y$ (primal feasibility) and

$$0 \in \{H z + h\} + \hat{\mathcal{N}}_{\mathcal{E}}(z) - \{\lambda\}, \quad (14a)$$

$$0 \in \hat{\mathcal{N}}_{\hat{\mathcal{N}}_{\mathcal{Z}}^*(z^\dagger) + \{z^\dagger\}}(y) + \{\lambda\}. \quad (14b)$$

By Lemma 3, (14b) is equivalent to (6b). Therefore, $(z^\dagger, \lambda^\dagger)$ also satisfies conditions (14). By strict convexity, implied by $H \succ 0$, $(z^\dagger, \lambda^\dagger)$ is primal-dual optimal for Problem (13). Furthermore, using Lemma 3, we know that there exists an $\epsilon > 0$ such that $z^\dagger \in \mathcal{Z} \cap \mathcal{B}_\epsilon(z^\dagger) \subseteq \hat{\mathcal{N}}_{\mathcal{Z}}^*(z^\dagger) + \{z^\dagger\}$, therefore, the pair $y = z = z^\dagger$ is also optimal for the non-convex program

$$\min_{z, y: z=y} \frac{1}{2} z^\top H z + h^\top z + \chi_{\mathcal{E} \times (\mathcal{Z} \cap \mathcal{B}_\epsilon(z^\dagger))}(z, y) \quad (15)$$

Problem (15) is a local instance of Problem (1), where the feasible region is restricted to $\mathcal{B}_\epsilon(z^\dagger)$. This implies that z^\dagger is locally optimal for Problem (2). \square

Theorem 1 implies that Algorithm 1 converges to local minima. We note that arbitrary global optimality tolerances can not be reached in general.

4.3 Existence

We have seen that for any regular KKT point we can ensure the existence of a ξ -proximal KKT point by choosing ξ large enough. Therefore, if there exists a regular KKT point, we can ensure the existence of fixed points of operator T_ξ , as demonstrated in the following theorem.

Theorem 2 (Existence of fixed points of T_ξ) *If there exists a regular KKT point $(z^\dagger, \lambda^\dagger)$ of Problem (2), then there exists a $\bar{\xi} > 0$ such that T_ξ has at least one fixed point for any $\xi \geq \bar{\xi}$.*

PROOF. *Given a regular KKT point $(z^\dagger, \lambda^\dagger)$ of Problem (2), and using Proposition 1(i), there exists a $\bar{\xi} > 0$ such that for any $\xi \geq \bar{\xi}$ we have that $(z^\dagger, \lambda^\dagger)$ is a ξ -proximal KKT point. Therefore, by Lemma 2, $s^\dagger := z^\dagger - \frac{1}{\xi} \lambda^\dagger \in \text{zero } K_\xi$ and thus s^\dagger is a fixed point of T_ξ . \square*

In Appendix A we illustrate three cases for the existence of KKT points, and also give an example where the operator T_ξ fails to have any fixed points.

4.4 Local convergence to local minima

In this section, we prove that the presented method converges locally to local minima. This proof is based on local properties of the projection operator \mathcal{P}_Z .

We say that a fixed point s° corresponds to a local minimum z° , if the ξ -proximal KKT point (z°, λ°) can be constructed from s° through (10). Note that, as shown in Lemma 2 and Theorem 1, any fixed point of T_ξ can be used to reconstruct a local minimum. We denote the set of fixed points corresponding to z° by

$$\text{fix } T_\xi|z^\circ := \{s \mid (z^\circ, \xi(z^\circ - s)) \text{ satisfies (7)}\}.$$

The sets $\text{fix } T_\xi|z^\circ$ are closed, convex, see [22, p. 213], and satisfy Proposition 2.

Proposition 2 *There exists a $\bar{\xi} > 0$ such that for any local optimum z° , $\text{fix } T_\xi|z^\circ$ is either*

- i) empty, for all $\xi \geq \bar{\xi}$, or*
- ii) a singleton set, for all $\xi \geq \bar{\xi}$, or*
- iii) it contains more than one element, for all $\xi \geq \bar{\xi}$.*

We make the following assumptions:

- (A1)** Problem (2) has at least one regular KKT point.
- (A2)** There exists a $\bar{\xi} > 0$ such that
 - (i) $\bar{\xi} > \lambda_{\min}^+(R)^{-1}$, i.e., (9a),
 - (ii) $\bar{\xi}$ satisfies Proposition 2, and

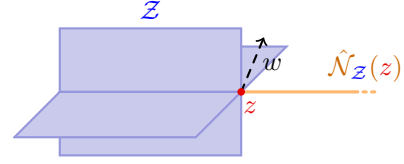


Fig. 3. A set Z where (A3) is violated at point z . We see that $w \in \hat{N}_Z(z)$, but $z + \epsilon w \notin Z$ for all $\epsilon > 0$.

(iii) for any local optimum z° , and any $\xi \geq \bar{\xi}$, for which $\text{fix } T_\xi|z^\circ \neq \emptyset$, there exists a fixed point $s^\circ \in \text{fix } T_\xi|z^\circ$ that satisfies $s^\circ \in \text{relint } \hat{N}_Z(z^\circ) + \{z^\circ\}$.

(A3) The structure of set Z is such that, for any $z \in Z$, either $\hat{N}_Z(z) = \{0\}$, or there exists an $\epsilon > 0$ such that for all $w \in \hat{N}_Z(z)^\perp \cap \mathcal{B}_\epsilon$, we have $z + w \in Z$.

We note that Assumptions (A1)–(A3) are substantially less restrictive than common assumptions for non-convex optimization methods such as smoothness or regularity of the constraints at critical points. Assumption (A1) ensures the existence of regular KKT points, avoiding degenerate cases. Together with the choice of $\xi \geq \bar{\xi}$ from Assumption (A2)(ii), it furthermore implies the existence of fixed points of T_ξ . In addition, the choice of $\xi \geq \bar{\xi}$ in Assumption (A2)(i) ensures that $\lambda_{\min}^+(M_\xi) > 1$ holds. Assumptions (A2)(i)–(ii) can always be fulfilled by a large enough choice of $\bar{\xi}$, whereas Assumption (A2)(iii) can be understood as a *non-degeneracy* condition on the multipliers. Finally, (A3) is an assumption on the geometry of Z . It is satisfied by the sets in Figure 2 and Figure A.1, whereas Figure 3 illustrates a simple counter-example in three dimensions. It is not clear whether (A3) holds for all problems of the form of Problem (3). However, it is possible to check numerically whether (A3) holds for a given set Z . In Appendix D we provide Algorithm 3 to check this assumption, and apply it to the numerical example in Section 5.

In Algorithm 1, we apply the Krasnoselskij iteration to the operator T_ξ . This iteration is known to converge *globally* when the operator T_ξ is non-expansive, which is the case when Z is convex. To show *local* convergence for the non-convex case, we need T_ξ to be non-expansive in a neighborhood around fixed points. Starting in such a neighborhood, we will converge via the same argument. This is detailed in Theorem 3. The local non-expansiveness of T_ξ can, similarly to the convex case, be shown via the local firm non-expansiveness of the projection operator \mathcal{P}_Z . Using Assumptions (A1)–(A3), in Lemma 4 we show that, in a neighborhood around almost all fixed points, the projection \mathcal{P}_Z behaves like a projection onto a convex set. Therefore, it is locally firmly non-expansive, single-valued and continuous [27, Proposition 4.8, p. 61]. Then, in Lemma 5, we use this property, together with the particular construction of the operator T_ξ , to show that T_ξ is non-expansive, single-valued and continuous in a neighborhood around almost all fixed points. This guarantees the *local convergence* of

Algorithm 1 to a *local minimum*, almost always.

Lemma 4 *Let Assumptions (A1)–(A3) hold. For any $\xi > \bar{\xi}$, and any local minimum z° to Problem (2) with $z^\circ \notin \text{fix } T_\xi$ and $\text{fix } T_\xi|z^\circ \neq \emptyset$; we have that for all fixed points $s^\circ \in \text{fix } T_\xi|z^\circ$, except a measure-zero subset, there exists an $\epsilon > 0$ such that the projection \mathcal{P}_Z is single-valued, continuous and firmly non-expansive on $\mathcal{B}_\epsilon(s^\circ)$.*

Lemma 5 *Let $\xi > 0$ and given any fixed point $s^\circ \in \text{fix } T_\xi$ such that there exists an $\epsilon > 0$, where the projection \mathcal{P}_Z is single-valued, continuous and firmly non-expansive on $\mathcal{B}_\epsilon(s^\circ)$. Then the operator T_ξ is also single-valued, continuous and non-expansive on $\mathcal{B}_\epsilon(s^\circ)$.*

Theorem 3 *Let Assumptions (A1)–(A3) hold. For any $\xi > \bar{\xi}$, and an initial iterate s_0 sufficiently close to a fixed point of T_ξ , Algorithm 1 converges almost always to a fixed point $s^\circ \in \text{fix } T_\xi$. When it converges, z_j and y_j converge to each other and a local minimum of Problem (2).*

PROOF. *Given (A2), let $\xi > \bar{\xi}$. Together with (A1), this implies the existence of fixed points of T_ξ , i.e., $\text{fix } T_\xi \neq \emptyset$. We first consider the case where there exists a fixed point $s^\circ \in \text{fix } T_\xi$ with corresponding local minimum z° such that $s^\circ = z^\circ$. This is the case, where $(z^\circ, 0)$ is a KKT point of Problem (2). Therefore*

$$\begin{aligned} M_\xi z^\circ + c_\xi &\in \mathcal{P}_Z(z^\circ) = \{z^\circ\} \\ \Leftrightarrow z^\circ &= (I - M_\xi)^{-1}c_\xi = \bar{v} - R(h + H\bar{v}), \end{aligned}$$

with $I - M_\xi$ invertible due to (A2)(i) and (9b). This is checked in step 1 of Algorithm 1, if it holds the algorithm terminates and returns z° , a global minimum. If there is no $s^\circ \in \text{fix } T_\xi$ such that the corresponding local minimum z° satisfies $s^\circ = z^\circ$, we can apply Lemma 4. It says that for any local minimum z° , such that $\text{fix } T_\xi|z^\circ \neq \emptyset$, we know ξ can be chosen large enough such that for all $s^\circ \in \text{fix } T_\xi|z^\circ$, except a measure-zero subset, there exists an $\epsilon > 0$ such that the projection \mathcal{P}_Z is single-valued, continuous and firmly-nonexpansive on $\mathcal{B}_\epsilon(s^\circ)$. We consider any such s° . Using Lemma 5, this means that T_ξ is non-expansive on $\mathcal{B}_\epsilon(s^\circ)$. Assuming the initial iterate is close enough, i.e., $s_0 \in \mathcal{B}_\epsilon(s^\circ)$, then by the non-expansiveness of T_ξ the iterates will satisfy $s_j \in \mathcal{B}_\epsilon(s^\circ)$ for all $j \geq 0$. The Krasnoselskij iteration applied to T_ξ , in step 5 of Algorithm 1, converges to a fixed point of T_ξ for any choice of step-size parameter $\gamma \in (0, 1)$ [24, Theorem 3.2, p. 65]. The single-valuedness, and continuity of T_ξ , and convergence $\lim_{j \rightarrow \infty} \|z_j - y_j\| = 0$, follows. By Theorem 1, z_j and y_j converge to a local minimum of Problem (2). \square

Theorem 3 may require ξ to be large. Moreover, a lower bound of ξ satisfying Assumption (A2) may be hard to compute. However, in practice, good results can be obtained for “small” values of ξ . In addition, if the algorithm fails to converge, the theoretical results indicate that choosing a larger value of ξ may improve the convergence behavior. This is verified experimentally in Section 5.2, where we examine the behavior for different ξ .

5 Numerical results

In this section, we apply the proposed method to a hybrid MPC problem for racing miniature cars [28], where the friction forces acting on the tires are modeled as a PWA function, see [29, p. 108ff]. The forward velocity v_x of the car is fixed to 2 m/s. The state $x = (v_y, \omega)$ of the system consists of the lateral velocity v_y and the turning rate ω . The steering angle δ is the only input to the system. The continuous-time dynamics are described by

$$\begin{aligned} \dot{v}_y &= \frac{1}{m}(F_{f,y}(v_y, \omega, \delta) + F_{r,y}(v_y, \omega) - mv_x\omega), \\ \dot{\omega} &= \frac{1}{I_Z}(l_f F_{f,y}(v_y, \omega, \delta) - l_r F_{r,y}(v_y, \omega)), \end{aligned}$$

where m, I_Z, l_f, l_r are known model parameters and $F_{f,y}, F_{r,y}$ are the lateral friction forces acting on the front and rear tires of the vehicle, respectively. They are given as PWA functions with 5 pieces each, leading to a total of 19 non-empty regions per time step. For a prediction horizon N , this leads to 19^N possible combinations overall – a large number. The dynamics are discretized with a sampling time of $T_s = 20$ ms. Additionally we impose input constraints $\delta \in [-23^\circ, 23^\circ]$ and state constraints:

$$v_y \in [-1 \text{ m/s}, 1 \text{ m/s}], \quad \omega \in [-8 \text{ rad/s}, 8 \text{ rad/s}]. \quad (16)$$

The objective is to track a state \bar{x} and input $\bar{\delta}$ reference trajectory producing an S-shaped motion of the race car.

$$\sum_{k=1}^N \|Q(x_{k+1} - \bar{x}_{k+1})\|^2 + \|R(\delta_k - \bar{\delta}_k)\|^2,$$

where $Q = \begin{pmatrix} 1 & 0 \\ 0 & \sqrt{10} \end{pmatrix}$ and $R = 1$.

We compare our method with an MIP reformulation based on disjunctions [20, Section 5], solved using CPLEX, Gurobi and MOSEK. We used YALMIP [30] to model the optimization problem. We further compare to an efficient implementation of non-convex ADMM, similar to [13], where the splitting (2) was used. Efficient C-code for the proposed method and ADMM was generated automatically using the developed code generation tool [18], integrating explicit solutions of the individual convex projections using MPT3 [26]. The resulting binaries are 490 kB for prediction horizon $N = 10$ and 550 kB for $N = 20$. The binaries for ADMM are of comparable size. In contrast, the executables for the MIP solvers are in the range of 10 to 20 MB. The reported timings are obtained on an Intel Core i7 processor *using a single core* running at 2.8 GHz. No warm-starting or re-starting is used and we always start with the initial iterate $s_0 = 0$ ($y_0 = \lambda_0 = 0$ for ADMM). We have used step size parameter $\gamma = 0.5$ and consensus tolerance $\epsilon_{\text{tol}} = 10^{-3}$. Assumption (A3) was verified to hold numerically, using Algorithm 3 in Appendix D.

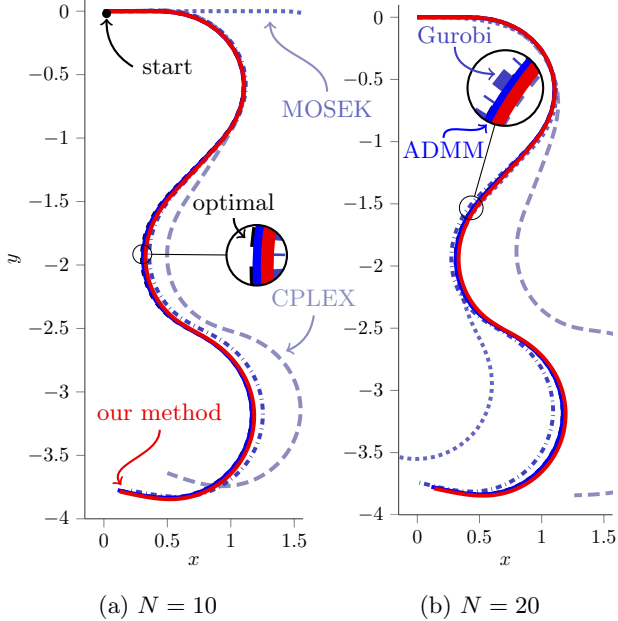


Fig. 4. Closed-loop position trajectory with initial condition $x = y = \varphi = 0$. Optimal closed-loop trajectory (**dashed**), our method (**solid**), ADMM (**solid**), CPLEX (**dashed**), Gurobi (**dash-dotted**) and MOSEK (**dotted**).

5.1 Closed-loop comparison

We consider closed-loop behavior, where the MPC is applied in a receding-horizon fashion. For every time step a problem with different initial state and reference is solved and only the first input u_1 is applied to the dynamical system. A new problem with updated initial state and reference is solved for the next time step. The MPC problem instances are solved for a prediction horizon of $N = 10$ ($\xi = 300$) and $N = 20$ ($\xi = 400$). The penalty parameter of ADMM was chosen to be $\rho = 350$ and $\rho = 450$ for $N = 10$ and $N = 20$, respectively. Tolerance ϵ_{tol} was also used for the termination criterion of ADMM, according to [12], as absolute, primal and dual residual tolerance. A time limit of 3 s for $N = 10$, and 85 s for $N = 20$ was imposed on all solvers. Both time limits are well above the computation times achieved by our algorithm, with a median runtime of 30 ms for $N = 10$, and 87 ms for $N = 20$, as reported in Figure 6. For $N = 20$, Gurobi has a median runtime of 8.5 s, reaching the time limit in some cases, while CPLEX and MOSEK reach the time limit for many time steps and have a median runtime close to 85 s. ADMM is slightly faster than our method, with a median runtime of 54 ms. However it fails to converge in a few cases, as shown in Figure 6. In contrast, our method converges in at most 1878 iterations for each of the 150 problems, solved in the closed-loop simulation. This is illustrated in Figure 5. We compare the closed-loop trajectories of the different methods over 150 steps. The initial state is $v_y = \omega = 0$. The dynamics of the system are with respect to the lateral and angular velocities, v_y and ω , with a fixed forward velocity $v_x = 2 \text{ m/s}$. We compare the position of

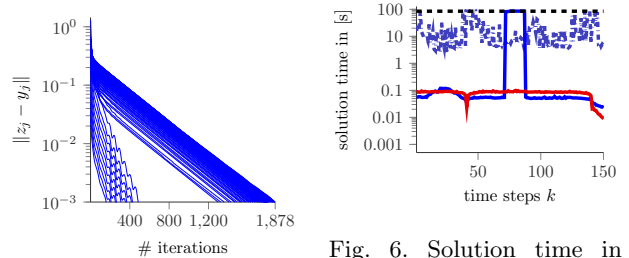


Fig. 5. Consensus violations $\|z_j - y_j\|$ for $N = 20$ and time steps 1 to 150, illustrating convergence.

Fig. 6. Solution time in [s] for time steps k of closed-loop simulation, with $N = 20$, time limit 85 s (**dashed**). Our method (**solid**), ADMM (**solid**), Gurobi (**dash-dotted**).

N	our method	ADMM	Gurobi	CPLEX	MOSEK
10	1.2%	1%	3.1%	14%	92%
20	1%	0.2%	5%	21%	34%

Table 1

Comparison of relative 2-norm distance $\frac{\|z - z^*\|}{\|z^*\|}$ to the optimal closed-loop position trajectory z^* for $N = 10, 20$.

the car, rather than the velocities, using the *position* dynamics to transform the velocities into positions, via integration of $\dot{\varphi} = \omega$, $\dot{x} = v_x \cos(\varphi) - v_y \sin(\varphi)$ and $\dot{y} = v_x \sin(\varphi) + v_y \cos(\varphi)$. The position trajectories are presented in Figure 4. The proposed method visibly outperforms the commercial MIP solvers in terms of solution quality. This is also illustrated in Table 1, where the relative distance to the optimal closed-loop trajectory is reported. Our method comes very close to the optimal trajectory, while requiring several orders of magnitude less runtime. Both our method and ADMM provide near optimal solutions for similar computational effort. However, our method additionally provides guarantees on the convergence properties of the algorithm.

5.2 Effect of proximal scaling

To better understand the proximal scaling ξ , we consider 2000 feasible, random instances with different initial conditions (v_y, ω) satisfying (16). We solve the MPC problem for 40 values of ξ , with a horizon of $N = 10$ and step size $\gamma = 0.95$. Figure 7 demonstrates the relationship between ξ and (i) the number of solved instance, and (ii) the number of iterations needed for convergence. For larger ξ more problems are solved, with only 4 unsolved problems remaining for $\xi = 5000$. Furthermore, the number of iterations needed to reach the consensus threshold (right axis) grows only modestly with larger ξ . In all instances, the constraint violations and relative suboptimality do not change significantly. These findings are consistent with our expectations from the theory, i.e., that larger ξ usually lead to more problems solved but at the expense of slower convergence.

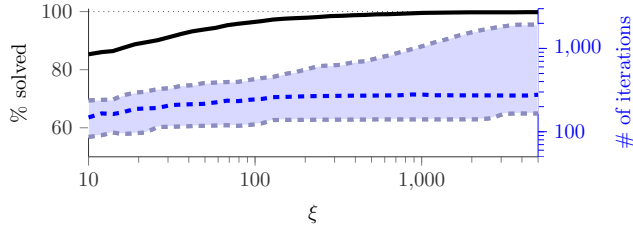


Fig. 7. Effect of proximal scaling ξ . Percentage of problems solved (solid, left axis) and number of iterations to reach 10^{-3} consensus violation (right axis) for the solved problems, median (dashed), 5-th and 95-th percentile (dashed).

6 Conclusion

We propose a low-complexity method for finding local minima of non-convex, non-smooth optimization problems. This simple and fast method is ideal for hybrid MPC on embedded platforms. In numerical experiments, we observe that our method provides near optimal solutions at a fraction of the time needed by global solvers. Moreover, it is competitive with ADMM in terms of speed. In contrast to other local methods, our algorithm additionally provides local optimality and local convergence guarantees.

Acknowledgements

We would like to thank the associate editor and reviewers for their time and helpful suggestions.

References

- [1] S. Di Cairano, A. Bemporad, I. Kolmanovsky, and D. Hrovat, "Model predictive control of magnetically actuated mass spring dampers for automotive applications," *International Journal of Control*, vol. 80, no. 11, pp. 1701–1716, 2007.
- [2] A. Arce, A. del Real, and C. Bordons, "MPC for battery/fuel cell hybrid vehicles including fuel cell dynamics and battery performance improvement," *Journal of Process Control*, vol. 19, no. 8, pp. 1289–1304, 2009.
- [3] T. Geyer, G. Papafotiou, R. Frasca, and M. Morari, "Constrained optimal control of the step-down dc-dc converter," *IEEE Transactions on Power Electronics*, vol. 23, no. 5, pp. 2454–2464, 2008.
- [4] M. Morari and J. Lee, "Model predictive control: past, present and future," *Computers & Chemical Engineering*, vol. 23, no. 4–5, pp. 667–682, 1999.
- [5] A. Bemporad and M. Morari, "Control of systems integrating logic, dynamics, and constraints," *Automatica*, vol. 35, no. 3, pp. 407–427, 1999.
- [6] IBM, "IBM ILOG CPLEX optimization studio," 2015.
- [7] A. Alessio and A. Bemporad, *A Survey on Explicit Model Predictive Control*, pp. 345–369. Springer Berlin Heidelberg, 2009.
- [8] D. Frick, A. Domahidi, and M. Morari, "Embedded optimization for mixed logical dynamical systems," *Computers & Chemical Engineering*, vol. 72, pp. 21–33, 2015.
- [9] D. Axehill, *Integer Quadratic Programming for Control and Communication*. PhD thesis, Linköping University, 2008.
- [10] S. Sager, *Numerical methods for mixed-integer optimal control problems*. PhD thesis, Universität Heidelberg, 2005.
- [11] M. Jung, *Relaxations and Approximations for Mixed-Integer Optimal Control*. PhD thesis, Universität Heidelberg, 2013.
- [12] S. Boyd, N. Parikh, E. Chu, B. Peleato, and J. Eckstein, "Distributed optimization and statistical learning via the alternating direction method of multipliers," *Foundations and Trends in Machine Learning*, vol. 3, pp. 1–122, 2011.
- [13] R. Takapoui, N. Moehle, S. Boyd, and A. Bemporad, "A simple effective heuristic for embedded mixed-integer quadratic programming," *arXiv preprint*, 2015.
- [14] G. Li and T. Pong, "Global convergence of splitting methods for nonconvex composite optimization," *SIAM Journal on Optimization*, vol. 25, no. 4, pp. 2434–2460, 2015.
- [15] S. Magnússon, P. C. Weeraddana, M. G. Rabbat, and C. Fischione, "On the convergence of alternating direction lagrangian methods for nonconvex structured optimization problems," *IEEE Transactions on Control of Network Systems*, vol. 3, no. 3, pp. 296–309, 2016.
- [16] J.-H. Hours and C. Jones, "A parametric nonconvex decomposition algorithm for real-time and distributed NMPC," *IEEE Transactions on Automatic Control*, vol. 61, no. 2, pp. 287–302, 2016.
- [17] B. Houska, J. Frasch, and M. Diehl, "An augmented lagrangian based algorithm for distributed nonconvex optimization," *SIAM Journal on Optimization*, vol. 26, no. 2, pp. 1101–1127, 2016.
- [18] D. Frick, "Automatic code-generation tool for LIM." <http://github.com/dafrick/codegen>, 2016.
- [19] J. Nocedal and S. Wright, *Numerical optimization*. Springer Science+Business Media, 2 ed., 2006.
- [20] J. Vielma, "Mixed integer linear programming formulation techniques," *SIAM Review*, vol. 57, no. 1, pp. 3–57, 2015.
- [21] A. Ruszczyński, *Nonlinear Optimization*. Princeton University Press, 2006.
- [22] R. Rockafellar and R. Wets, *Variational analysis*. Springer, 1998.
- [23] R. Henrion and J. Outrata, "On calculating the normal cone to a finite union of convex polyhedra," *Optimization*, vol. 57, no. 1, pp. 57–78, 2008.
- [24] V. Berinde, *Iterative approximation of fixed points*. Springer, 2 ed., 2007.
- [25] A. Domahidi, A. Zraggen, M. Zeilinger, M. Morari, and C. Jones, "Efficient interior point methods for multistage problems arising in receding horizon control," in *IEEE Conference on Decision and Control*, pp. 668–674, 2012.
- [26] M. Herceg, M. Kvasnica, C. Jones, and M. Morari, "Multi-parametric toolbox 3.0," in *European Control Conference*, pp. 502–510, 2013.
- [27] H. Bauschke and P. Combettes, *Convex analysis and monotone operator theory in Hilbert spaces*. Springer, 2011.
- [28] A. Liniger, A. Domahidi, and M. Morari, "Optimization-based autonomous racing of 1:43 scale RC cars," *Optimal Control Applications and Methods*, vol. 36, pp. 628–647, 2015.
- [29] A. Hempel, *Control of Piecewise Affine Systems Through Inverse Optimization*. PhD thesis, ETH Zürich, 2015. Dissertation, ETH-Zürich, 2015, No. 23222.
- [30] J. Löfberg, "YALMIP : a toolbox for modeling and optimization in MATLAB," in *IEEE International Symposium on Computer Aided Control Systems Design*, pp. 284–289, 2004.

- [31] J. Ye, “Constraint qualifications and necessary optimality conditions for optimization problems with variational inequality constraints,” *SIAM Journal on Optimization*, vol. 10, no. 4, pp. 943–962, 2000.
- [32] G. Dantzig, *Linear programming and extensions*. Princeton University Press, 1963.

A Examples regarding existence of fixed points

In Figure A.1 we illustrate three cases for the existence and nature of KKT points, and also give an example where the operator T_ξ fails to have any fixed points. Figures A.1a–A.1c are cases where the proximal scaling ξ can be chosen such that fixed points of T_ξ exists. Figures A.1a and A.1b illustrate common cases. On the other hand Figure A.1c depicts a more rare case where both regular as well as multipliers that are not regular, exist for the same optimum. In all of these three cases existence is ensured for any $\xi > 0$ and we may find local minima using the proposed method. Finally, Figure A.1d illustrates a degenerate case where the feasible set is a singleton and none of its corresponding KKT points are regular. In this case operator T_ξ would not have a fixed point for any $\xi > 0$, even though a (generalized) KKT point exists.

B Simple hybrid MPC example

We consider a simple example taken from the hybrid MPC literature [5, Example 4.1, p. 415]. It consists of two states, one input and PWA dynamics defined over two regions:

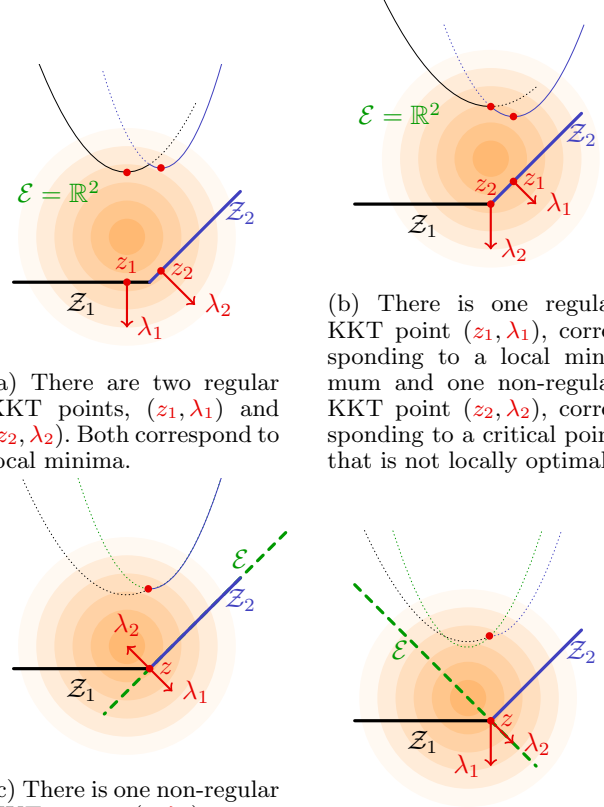
$$x_{k+1} = \begin{cases} A_1 x_k + B u_k & \text{if } x_{k,1} \geq 0 \\ A_2 x_k + B u_k & \text{if } x_{k,1} \leq 0 \end{cases},$$

with $u_k \in [-1, 1]$ and

$$A_1 = \frac{2}{5} \begin{pmatrix} 1 & -\sqrt{3} \\ \sqrt{3} & 1 \end{pmatrix}, A_2 = \frac{2}{5} \begin{pmatrix} 1 & \sqrt{3} \\ -\sqrt{3} & 1 \end{pmatrix}, B = \begin{pmatrix} 0 \\ 1 \end{pmatrix},$$

and a regulation objective $\sum_{k=1}^N \|x_{k+1}\|^2 + \|u_k\|^2$. We compare our method under the same conditions as in Section 5. Automatically generated code results in binaries of at most 75 kB in size. Furthermore, assumption (A3) holds and has been verified using Algorithm 3 in Appendix D.

The problem is solved for different prediction horizons $N = 5, 10, 20, \dots, 60$. We choose $\xi = 10$ for all cases. The penalty parameter for ADMM is $\rho = 10$ and the same termination criterion as in Section 5 is used. Furthermore, a time limit of $t_{\max} = 1800$ s (30 minutes) is imposed for all solvers. The convergence of our method is illustrated in Figure B.1a. For $N = 40$ and the first time step it shows a decreasing consensus violation $\|z_j - y_j\|$. Even though not shown, the method also converges for all successive time steps (and horizons N), with similar convergence characteristics. This leads to a stable



(a) There are two regular KKT points, (z_1, λ_1) and (z_2, λ_2) . Both correspond to local minima.

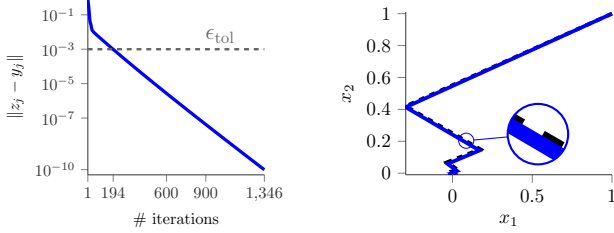
(b) There is one regular KKT point (z_1, λ_1) , corresponding to a local minimum and one non-regular KKT point (z_2, λ_2) , corresponding to a critical point that is not locally optimal.

(c) There is one non-regular KKT point (z, λ_1) corresponding to the unique global minimum. However (z, λ_2) is a regular KKT point that corresponds to the same global minimum.

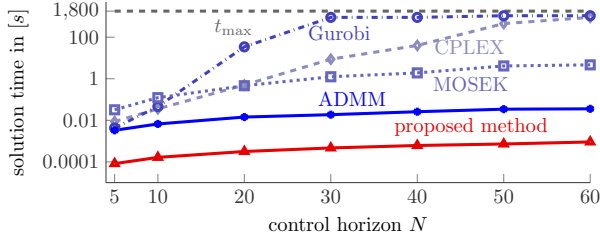
(d) There are only two KKT points (z, λ_1) and (z, λ_2) corresponding to the unique global minimum, both are non-regular.

Fig. A.1. Illustration of KKT points of the problem $\min_{z,y \in \mathcal{E} \times (\mathcal{Z}_1 \cup \mathcal{Z}_2)} \frac{1}{2} z^\top z + h^\top z$ s.t. $z = y$. The **level curves** of the objective are given and the objective value evaluated on \mathcal{Z}_1 , \mathcal{Z}_2 and \mathcal{E} is shown in the respective colors. It is solid where feasible, and dotted where infeasible. KKT points represent global or local minima, and critical points.

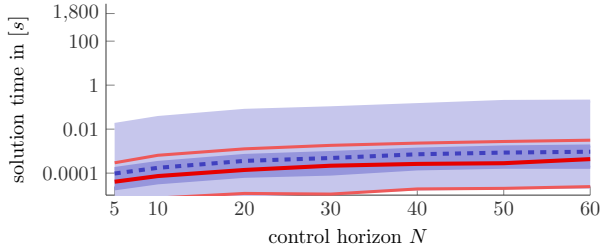
closed-loop trajectory, illustrated in Figure B.1b. The trajectory is almost indistinguishable from the optimum, obtained using a MIP reformulation based on disjunctions [20, Section 5]. The computational advantage of our method is underlined by Figure B.1c, where the average runtime for different control horizons N is shown. Our method is several orders of magnitude faster than the considered commercial MIP solvers. This difference becomes more pronounced for larger prediction horizons N . In fact, Gurobi (for $N \geq 30$) and CPLEX (for $N \geq 50$) frequently exceed the time limit. Our method also has substantially better average runtime than ADMM. This is because ADMM fails to converge for two of the ten time steps and terminates when it reaches 10'000 iterations. We were not able to achieve convergence of ADMM by adjusting ρ . If the median runtime is considered, then the proposed method is still slightly faster than ADMM as illustrated in Figure B.1d.



(a) Consensus violation $\|z_j - y_j\|$ (solid) for $N = 40$ at the first time step, with threshold (dashed). (b) Closed-loop trajectory, for $N = 40$ and 10 time steps. Optimal (dashed), and our method (solid).



(c) Average solution time in [s] for different control horizons. Our method (solid, \triangle), ADMM (solid, $*$) and a MIP reformulation solved using CPLEX (dashed, \diamond), Gurobi (dash-dotted, \circ) and MOSEK (dotted, \square).



(d) Min., max. and median solution time in [s] for our method (solid) with different control horizons. In comparison to the median solution time of ADMM (dashed), 25-th to 75-th percentile (light) and 5-th to 95-th percentile (very light).

Fig. B.1. Comparison of Example B with $\xi = 10$, $\gamma = 0.5$ and $\epsilon_{\text{tol}} = 10^{-3}$. The initial state is $x_1 = x_2 = 1$.

B.1 Local convergence to local minima

In order to illustrate the local convergence behavior of Algorithm 1, we have solved Example B for $N = 10$ and 50'000 different initial iterates $s_0 := z_0 - \xi^{-1}\lambda_0$, where z_0 was drawn uniformly randomly from $[-1, 1]^{50}$ and λ_0 from $[-10, 10]^{50}$. The proximal scaling was chosen as $\xi = 100$ and the consensus tolerance was $\epsilon_{\text{tol}} = 10^{-8}$. Algorithm 1 converges in 99.1% of cases. The local convergence of our algorithms can be seen in Figure B.3 where we have illustrated the percentage of initial iterates achieving certain objective values which correspond to local optima. In Figure B.3, we cluster the solutions into four clusters (a)–(d). The state trajectories of the solutions for each cluster are plotted in Figures B.2a–B.2d. Each cluster contains multiple local minima that have similar objective value. The 50'000 different initial

iterates only lead to 34 trajectories that each differ (in terms of the objective value) by at least 10^{-5} . Cluster (a) with 62.1% of initial iterates contains solutions that are very close to the global optimum. The initial iterate $s_0 = 0$ used in Example B belongs to this cluster. This illustrates that the presented method is indeed a local method, and does not converge to the global optimum, in general.

C Auxiliary propositions & proofs

In this section we use the following additional notation: The *relative boundary* of a set \mathcal{C} is $\text{relbd}\mathcal{C} := \text{cl}\mathcal{C} \setminus \text{relint}\mathcal{C}$, where $\text{cl}\mathcal{C}$ is the *closure* and $\text{relint}\mathcal{C}$ the *relative interior*.

We start with a proof sketch for Lemma 1 utilizing [31].

Proof sketch of Lemma 1 It can be shown that Problem (2) satisfies a regularity condition called a local error bound [31, Theorem 4.3, p. 952], which means the error due to a perturbation of the constraint set can be bounded in a particular way. Therefore applying [31, Proposition 4.2, p. 951] implies that Problem (2) is calm at every local solution, a regularity property of the optimization problem. Then using the calmness and [31, Theorem 3.6, p. 950] we obtain that for every local solution z° to Problem (2) there exists a $\lambda^\circ \in \mathbb{R}^n$ such that $(z^\circ, z^\circ, \lambda^\circ)$ is a KKT point of Problem (2). \square

To prove Proposition 1, we first elaborate on the structure of the regular normal cone of \mathcal{Z} , where the representation (C.1) is used.

$$\mathcal{Z} = \bigcup_{i=1}^I \mathcal{Z}^i, \quad (\text{C.1})$$

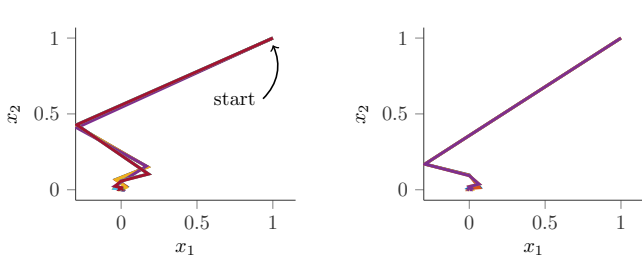
Proposition C.1 states, that the regular normal cone of \mathcal{Z} at z can be written as the finite intersection of the normal cones of its convex polyhedral parts \mathcal{Z}^i , where only the sets \mathcal{Z}^i that contain z (i.e. the active components of \mathcal{Z} at z) need to be considered.

Proposition C.1 ([23, p. 59f]) *The regular normal cone $\hat{\mathcal{N}}_{\mathcal{Z}}$ of \mathcal{Z} evaluated at $z \in \mathcal{Z}$ is given by*

$$\hat{\mathcal{N}}_{\mathcal{Z}}(z) = \bigcap_{i \in \mathcal{I}_{\mathcal{Z}}(z)} \hat{\mathcal{N}}_{\mathcal{Z}^i}(z).$$

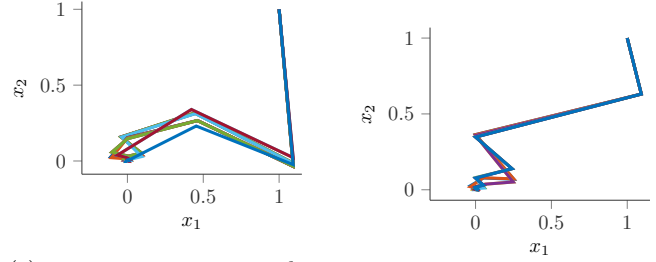
This allows us to prove Proposition 1.

Proof of Proposition 1 We consider the two statements separately.



(a) 7 trajectories with objective value in $[0.4189, 0.4225]$ obtained from 62.1% of initial iterates s_0 .

(b) 4 trajectories with objective value in $[0.5072, 0.5078]$ obtained from 15.2% of initial iterates s_0 .



(c) 15 trajectories with objective value in $[0.9411, 0.9748]$ obtained from 21% of initial iterates s_0 .

(d) 8 trajectories with objective value in $[1.5488, 1.5572]$ obtained from 0.9% of initial iterates s_0 .

Fig. B.2. Solutions obtained using 50'000 random initial iterates s_0 , of which 99.1% converged.

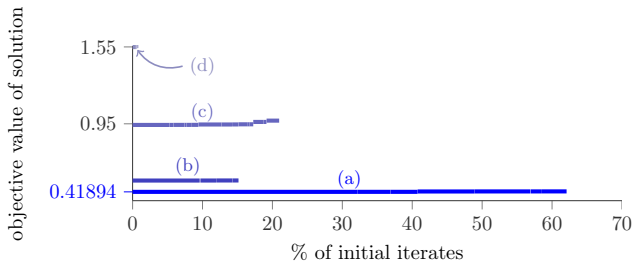


Fig. B.3. Percentage of initial iterates achieving certain objective values. Solutions are clustered into four clusters (a)–(d): 61.2% of solutions with objective values in $[0.4189, 0.4225]$ (a) with the **optimal objective 0.4189**, 15.2% with objective values in $[0.5072, 0.5078]$ (b), 21% with objective values in $[0.9411, 0.9748]$ (c) and 0.9% with objective values in $[1.5488, 1.5572]$ (d).

i) By definition, a regular KKT point (z, λ) satisfies $-\lambda \in \hat{\mathcal{N}}_{\mathcal{Z}}(z)$. We then have by Proposition C.1

$$-\lambda \in \hat{\mathcal{N}}_{\mathcal{Z}}(z) \Rightarrow -\lambda \in \bigcap_{i \in \mathcal{I}_{\mathcal{Z}}(z)} \hat{\mathcal{N}}_{\mathcal{Z}^i}(z). \quad (\text{C.2a})$$

For any $\xi > 0$ this is equivalent to

$$\begin{aligned} (\text{C.2a}) &\Leftrightarrow -\frac{1}{\xi}\lambda \in \hat{\mathcal{N}}_{\mathcal{Z}^i}(z) \quad \forall i \in \mathcal{I}_{\mathcal{Z}}(z) \\ &\Leftrightarrow z \in \mathcal{P}_{\mathcal{Z}^i}(z - \frac{1}{\xi}\lambda) \quad \forall i \in \mathcal{I}_{\mathcal{Z}}(z), \end{aligned} \quad (\text{C.2b})$$

where (C.2b) follows from the convexity of \mathcal{Z}^i and the relationship between the projection $\mathcal{P}_{\mathcal{Z}^i}$ and the normal cone $\hat{\mathcal{N}}_{\mathcal{Z}^i}$, described in [22, p. 212f]. By construction for any $\epsilon > 0$ small enough, we have $\mathcal{Z} \cap \mathcal{B}_{\epsilon}(z) = \bigcap_{i \in \mathcal{I}_{\mathcal{Z}}(z)} \mathcal{Z}^i \cap \mathcal{B}_{\epsilon}(z)$ and thus (C.2b) $\Rightarrow z \in \mathcal{P}_{\mathcal{Z} \cap \mathcal{B}_{\epsilon}(z)}(z - \frac{1}{\xi}\lambda)$. We now consider $\bar{\xi} = \frac{2}{\epsilon}\|\lambda\|$. For any $\xi \geq \bar{\xi}$ we have $\|(z - \frac{1}{\xi}\lambda) - z\| = \frac{1}{\xi}\|\lambda\| \leq \frac{\epsilon}{2}$ and therefore for all $x \in \mathcal{Z}$ with $\|z - x\| > \epsilon$ we have $\|(z - \frac{1}{\xi}\lambda) - x\| > \frac{\epsilon}{2}$. Together with $z \in \mathcal{P}_{\mathcal{Z} \cap \mathcal{B}_{\epsilon}(z)}(z - \frac{1}{\xi}\lambda)$, this implies that $z \in \mathcal{P}_{\mathcal{Z}}(z - \frac{1}{\xi}\lambda)$ for all $\xi \geq \bar{\xi} = \frac{2}{\epsilon}\|\lambda\|$, which implies that (z, λ) is a ξ -proximal KKT point.

ii) Given any $\xi > 0$, and any ξ -proximal KKT point (z, λ) . By definition $z \in \mathcal{P}_{\mathcal{Z}}(z - \frac{1}{\xi}\lambda)$ which implies $-\frac{1}{\xi}\lambda \in \hat{\mathcal{N}}_{\mathcal{Z}}(z)$ via [22, Example 6.16, p. 212]. This is equivalent to $-\lambda \in \hat{\mathcal{N}}_{\mathcal{Z}}(z)$, which directly implies that (z, λ) is a regular KKT point. \square

Proof of Lemma 2 Given any $\xi > 0$, and any $s^\dagger \in \text{zero } K_\xi$, by definition $0 \in \{M_\xi s^\dagger + c_\xi\} - \mathcal{P}_{\mathcal{Z}}(s^\dagger)$, and thereby $z^\dagger := M_\xi s^\dagger + c_\xi \in \mathcal{P}_{\mathcal{Z}}(s^\dagger)$. We define $\lambda^\dagger := \xi(z^\dagger - s^\dagger)$ and thus $z^\dagger \in \mathcal{P}_{\mathcal{Z}}(z^\dagger - \frac{1}{\xi}\lambda^\dagger) \Leftrightarrow (7b)$ holds. Furthermore, we $z^\dagger = M_\xi(z^\dagger - \frac{1}{\xi}\lambda^\dagger) + c_\xi$ which, using (8b)–(8d), is equivalent to $z^\dagger = R(\lambda^\dagger - h - H\bar{v}) + \bar{v}$. By strict convexity z^\dagger is the unique solution to

$$\begin{aligned} 0 &\in \partial_z(\frac{1}{2}z^\top H z + h^\top z - \lambda^\dagger{}^\top z + \chi_{\mathcal{E}}(z))(z^\dagger) \\ &\Leftrightarrow 0 \in \{H z^\dagger + h - \lambda^\dagger\} + \hat{\mathcal{N}}_{\mathcal{E}}(z^\dagger) \\ &\Leftrightarrow (7a) \text{ holds} \end{aligned}$$

Therefore $(z^\dagger, \lambda^\dagger)$ is a ξ -proximal KKT point if and only if $s^\dagger = z^\dagger - \frac{1}{\xi}\lambda^\dagger \in \text{zero } K_\xi$. \square

Proof of Lemma 3 We prove the two parts individually.

i) Take any $\bar{z} \in \mathcal{Z}$ and $z \in \mathcal{Z} \cap \mathcal{B}_\epsilon(\bar{z})$. Then using the definition of the polar cone we have that $z \in \hat{\mathcal{N}}_{\mathcal{Z}}^*(\bar{z}) + \{\bar{z}\}$ if and only if $\langle z - \bar{z}, v \rangle \leq 0, \forall v \in \hat{\mathcal{N}}_{\mathcal{Z}}(\bar{z})$. We assume for the sake of contradiction that for all $\bar{\epsilon} > 0$ there exists a $v \in \hat{\mathcal{N}}_{\mathcal{Z}}(\bar{z})$ such that $\langle z - \bar{z}, v \rangle > 0$. Using Proposition C.1, we have that for any $\bar{\epsilon} > 0$ small enough $v \in \hat{\mathcal{N}}_{\mathcal{Z}}(\bar{z})$ is equivalent to $\langle v, u - \bar{z} \rangle \leq 0$ for all $u \in \mathcal{Z}^i$, and all $i \in \mathcal{I}_{\mathcal{Z}}(\bar{z})$. However, since $z \in \mathcal{Z}^i$, and therefore by choosing $u = z$ we have $\langle v, u - \bar{z} \rangle < \langle z - \bar{z}, v \rangle$ – a contradiction. For any $\epsilon \in (0, \bar{\epsilon}]$ we can arrive at a contradiction in the same way.

ii) From [22, Corollary 6.21, p. 216] we know that since for any $z \in \mathcal{Z}$, $\hat{\mathcal{N}}_{\mathcal{Z}}(z)$ is closed and convex we have that $\hat{\mathcal{N}}_{\mathcal{Z}}(z) = \hat{\mathcal{N}}_{\mathcal{Z}}^{**}(z)$. Using the definition of the polar and regular normal cones [22, P. 203, p. 215], and convexity of $\hat{\mathcal{N}}_{\mathcal{Z}}^*(z)$ we have that $v \in \hat{\mathcal{N}}_{\mathcal{Z}}(z)$ is equivalent to

$$\begin{aligned} \langle v, w \rangle &\leq 0, & \forall w \in \hat{\mathcal{N}}_{\mathcal{Z}}^*(z) \\ \Leftrightarrow \langle v, u - z \rangle &\leq 0, & \forall u \in \hat{\mathcal{N}}_{\mathcal{Z}}^*(z) + \{z\} \\ \Leftrightarrow v &\in \hat{\mathcal{N}}_{\hat{\mathcal{N}}_{\mathcal{Z}}^*(z) + \{z\}}(z). & \square \end{aligned}$$

Proof of Proposition 2 Given any local optimum z° and $\bar{\xi} > 0$. We show that, the sets $\text{fix } T_\xi|_{z^\circ}$ can only grow with growing ξ . This means that the set $\text{fix } T_\xi|_{z^\circ}$ either (i) remains empty for all ξ , (ii) acquires a single element for some ξ and stays a singleton for all larger ξ , or (iii) does not stay a singleton. Given a $\bar{\xi}$ and $\xi \geq \bar{\xi}$, we will show that for any element $\bar{s} \in \text{fix } T_{\bar{\xi}}|_{z^\circ}$ there, uniquely, exists an element $s \in \text{fix } T_\xi|_{z^\circ}$. Consider any $\bar{s} \in \text{fix } T_{\bar{\xi}}|_{z^\circ}$, by definition and Lemma 2, it holds that (z°, λ) , with $\lambda := \xi(z^\circ - \bar{s})$, is a $\bar{\xi}$ -proximal KKT point. From Proposition 1, it further follows that (z°, λ) is also a ξ -proximal KKT point for any $\xi \geq \bar{\xi}$. Therefore, by definition, $s := z^\circ - \frac{1}{\xi}\lambda \in \text{fix } T_\xi|_{z^\circ}$. This means the sets $\text{fix } T_\xi|_{z^\circ}$ can only grow with larger ξ , and the result follows. \square

The following proposition is an auxiliary proposition needed to prove Lemma 4. It gives a local characterization of the projection around points \bar{s} where it is unique. It states, that there always exists a neighborhood $\mathcal{B}_\epsilon(\bar{s})$, with $\epsilon > 0$, such that for all points in the neighborhood the projection onto \mathcal{Z} can be restricted to the projection onto just the union of the active components of \mathcal{Z} at $\bar{z} := \mathcal{P}_{\mathcal{Z}}(\bar{s})$. Furthermore for all points $s \in \mathcal{B}_\epsilon(\bar{s})$ in the neighborhood the result $z \in \mathcal{P}_{\mathcal{Z}}(s)$ of the projection satisfies the bound $\|z - \bar{z}\| \leq \|s - \bar{s}\|$, i.e., the projection is locally non-expansive with respect to points where it is unique.

Proposition C.2 (Projection) *Given \bar{z} and \bar{s} such that $\mathcal{P}_{\mathcal{Z}}(\bar{s}) = \{\bar{z}\}$, then there exists an $\epsilon > 0$ such that for all $s \in \mathcal{B}_\epsilon(\bar{s})$*

$$\mathcal{P}_{\mathcal{Z}}(s) = \mathcal{P}_{\mathcal{Y}(\bar{z})}(s) \subseteq \mathcal{B}_{\|s - \bar{s}\|}(\bar{z}),$$

where

$$\mathcal{Y}(z) := \bigcup_{i \in \mathcal{I}_{\mathcal{Z}}(z)} \mathcal{Z}^i.$$

PROOF. First, we will show that for all $s \in \mathbb{R}^n$

$$\mathcal{P}_{\mathcal{Y}(\bar{z})}(s) \subseteq \mathcal{B}_{\|s - \bar{s}\|}(\bar{z}). \quad (\text{C.3a})$$

We have that for all $i \in \mathcal{I}_{\mathcal{Z}}(\bar{z})$, the projection $\mathcal{P}_{\mathcal{Z}^i}$ is non-expansive because \mathcal{Z}^i is closed and convex, therefore for any $i \in \mathcal{I}_{\mathcal{Z}}(\bar{z})$ and any $s \in \mathbb{R}^n$: $\|\mathcal{P}_{\mathcal{Z}^i}(s) - \mathcal{P}_{\mathcal{Z}^i}(\bar{s})\| \leq \|s - \bar{s}\|$. We consider any $z \in \mathcal{P}_{\mathcal{Y}(\bar{z})}(s)$. Since \bar{z} and \bar{s} are such that $\mathcal{P}_{\mathcal{Z}}(\bar{s}) = \{\bar{z}\}$ it follows that $\mathcal{P}_{\mathcal{Y}(\bar{z})}(\bar{s}) = \mathcal{P}_{\mathcal{Z}^i}(\bar{s}) = \{\bar{z}\}$ for all $i \in \mathcal{I}_{\mathcal{Z}}(\bar{z})$. In particular for some $i \in \mathcal{I}_{\mathcal{Z}}(\bar{z})$ we have that

$$\|z - \bar{z}\| = \|\mathcal{P}_{\mathcal{Z}^i}(s) - \mathcal{P}_{\mathcal{Z}^i}(\bar{s})\| \leq \|s - \bar{s}\|, \quad (\text{C.3b})$$

which implies (C.3a).

Second, we show that there exists an $\epsilon > 0$ such that for any $y \in \mathcal{Z} \setminus \mathcal{Y}(\bar{z})$

$$\|y - s\| > \|z - s\| \quad \forall s \in \mathcal{B}_\epsilon(\bar{s}), z \in \mathcal{P}_{\mathcal{Y}(\bar{z})}(s). \quad (\text{C.4a})$$

We define

$$\varsigma := \inf_{y \in \mathcal{Z} \setminus \mathcal{Y}(\bar{z})} \|y - \bar{s}\| - \|\bar{z} - \bar{s}\| > 0, \quad (\text{C.4b})$$

by closedness of \mathcal{Z} and \mathcal{Z}^i . The triangle inequality implies that for any $y \in \mathcal{Z} \setminus \mathcal{Y}(\bar{z})$ we have $\|y - \bar{s}\| \leq \|y - s\| + \|s - \bar{s}\|$. We choose $\epsilon < \frac{\varsigma}{3}$, which implies

$$\begin{aligned} \|y - s\| &\geq \|y - \bar{s}\| - \|s - \bar{s}\| \\ &\geq \varsigma + \|\bar{z} - \bar{s}\| - \|s - \bar{s}\| \\ &> 3\epsilon + \|\bar{z} - \bar{s}\| - \epsilon, \end{aligned} \quad (\text{C.4c})$$

where in the second step we have used (C.4b), and in the third step we have used $\varsigma > 3\epsilon$ and $\|s - \bar{s}\| \leq \epsilon$. Now we consider any $z \in \mathcal{P}_{\mathcal{Y}(\bar{z})}(s)$, via the triangle inequality $\|z - s\| \leq \|z - \bar{z}\| + \|s - \bar{s}\| + \|\bar{z} - \bar{s}\|$ and therefore by using (C.3b)

$$\|z - s\| \leq 2\|s - \bar{s}\| + \|\bar{z} - \bar{s}\| \leq 2\epsilon + \|\bar{z} - \bar{s}\|,$$

which together with (C.4c) implies (C.4a). (C.3a) and (C.4a) then imply the result. \square

In order to prove Lemma 4, we make the following claim:

Claim 1 *Given Assumptions (A1)–(A2). For any $\xi \geq \bar{\xi}$ and any local minimum z° to Problem (2), with $\text{fix } T_\xi|_{z^\circ} \neq \emptyset$ and $z^\circ \notin \text{fix } T_\xi$, we have that*

$$\mathcal{P}_{\mathcal{Z}}(s^\circ) = \{z^\circ\}, \text{ and} \quad (\text{C.5a})$$

$$s^\circ \in \text{relint } \hat{\mathcal{N}}_{\mathcal{Z}}(z^\circ) + \{z^\circ\}, \quad (\text{C.5b})$$

for all fixed points $s^\circ \in \text{fix } T_\xi|_{z^\circ}$, except a measure zero subset.

We will show Claim 1 right after the proof of Lemma 4.

Proof of Lemma 4 We assume that Claim 1 holds, and consider any pair z°, s° satisfying (C.5). We will show

that in a neighborhood of s° the projection onto \mathcal{Z} is the same as projecting onto an appropriate closed, convex set. This then implies local firm non-expansiveness, continuity and single-valuedness due to the properties of projections onto closed, convex sets.

Let $\mathcal{B}_\epsilon(s^\circ)$ be a neighborhood of s° , for some $\epsilon > 0$ small enough. We define two linear subspaces $\mathcal{S} := \text{lin}(\hat{\mathcal{N}}_{\mathcal{Z}}(z^\circ))$, the linear subspace spanned by $\hat{\mathcal{N}}_{\mathcal{Z}}(z^\circ)$, and its orthogonal complement \mathcal{S}^\perp . Clearly, for any $s \in \mathcal{B}_\epsilon(s^\circ)$ we can write $s = s^\circ + u + v$, where $u \in \mathcal{S}$, $v \in \mathcal{S}^\perp$ and $u + v \in \mathcal{B}_\epsilon$. This decomposition allows us to argue about the contribution of u and v successively. We consider $\bar{s} := s^\circ + u$. Due to $\mathcal{P}_{\mathcal{Z}}(s^\circ) = \{z^\circ\}$ and [22, Example 6.16, p. 212], we have $\mathcal{P}_{\mathcal{Z}}(\bar{s}) = \mathcal{P}_{\mathcal{Z}}(s^\circ + u) = \{z^\circ\}$ for all $u \in \mathcal{B}_\epsilon$. Furthermore, due to openness of $\text{relint } \hat{\mathcal{N}}_{\mathcal{Z}}(z^\circ)$ on \mathcal{S} , we have that for $\epsilon > 0$ small enough $\bar{s} := s^\circ + u$ satisfies $\bar{s} \in \text{relint } \hat{\mathcal{N}}_{\mathcal{Z}}(z^\circ) + \{z^\circ\}$ for all $u \in \mathcal{B}_\epsilon$. Therefore instead of considering a pair z°, s° satisfying (C.5), we will consider z°, \bar{s} . Now we look at the contribution of v , i.e., $s = \bar{s} + v$. Similarly to Lemma 3, where we showed that we can replace the regular normal cone of \mathcal{Z} by the normal cone of $\hat{\mathcal{N}}_{\mathcal{Z}}^*(z^\circ) + \{z^\circ\}$, we will now consider the projection onto that set. We do this because in some sense $\hat{\mathcal{N}}_{\mathcal{Z}}^*(z^\circ) + \{z^\circ\}$ is a local convexification of \mathcal{Z} . We notice that $v \in \hat{\mathcal{N}}_{\mathcal{Z}}^*(z^\circ)$, since $v \in \mathcal{S}^\perp \subseteq \hat{\mathcal{N}}_{\mathcal{Z}}^*(z^\circ)$ by definition. Next, we consider the projection $\mathcal{P}_{\hat{\mathcal{N}}_{\mathcal{Z}}^*(z^\circ)}(s - z^\circ)$:

$$\begin{aligned} & \arg \min_{w \in \hat{\mathcal{N}}_{\mathcal{Z}}^*(z^\circ)} \|\bar{s} - z^\circ + v - w\|^2 \\ &= \arg \min_{w \in \hat{\mathcal{N}}_{\mathcal{Z}}^*(z^\circ)} \|\bar{s} - z^\circ\|^2 + \|v - w\|^2 - 2\langle \bar{s} - z^\circ, w \rangle \end{aligned}$$

Where we have used that $\langle \bar{s} - z^\circ, v \rangle = 0$. Since $\langle \bar{s} - z^\circ, w \rangle \leq 0$, we immediately see that v is a minimizer. It is unique because the set $\hat{\mathcal{N}}_{\mathcal{Z}}^*(z^\circ)$ is closed and convex, therefore $\mathcal{P}_{\hat{\mathcal{N}}_{\mathcal{Z}}^*(z^\circ)}(s - z^\circ) = \{v\}$ and consequently

$$\mathcal{P}_{\hat{\mathcal{N}}_{\mathcal{Z}}^*(z^\circ) + \{z^\circ\}}(\bar{s} + v) = \{z^\circ + v\}.$$

Additionally, due to $\mathcal{Z} \cap \mathcal{B}_\epsilon(z^\circ) \subseteq \hat{\mathcal{N}}_{\mathcal{Z}}^*(z^\circ) + \{z^\circ\}$ from Lemma 3 and $z^\circ + v \in \mathcal{Z} \cap \mathcal{B}_\epsilon(z^\circ)$ due to Assumption (A3), it follows that $\{z^\circ + v\} \in \mathcal{P}_{\mathcal{Z}}(\bar{s} + v)$. Finally using Proposition C.2 we know that

$$\mathcal{P}_{\mathcal{Z}}(\bar{s} + v) \subseteq \mathcal{Z} \cap \mathcal{B}_{\|v\|}(z^\circ) \subseteq \mathcal{Z} \cap \mathcal{B}_\epsilon(z^\circ),$$

which immediately implies that

$$\mathcal{P}_{\mathcal{Z}}(\bar{s} + v) = \mathcal{P}_{\hat{\mathcal{N}}_{\mathcal{Z}}^*(z^\circ) + \{z^\circ\}}(\bar{s} + v) = \{z^\circ + v\}.$$

This means for all $s \in \mathcal{B}_\epsilon(s^\circ)$ the projection onto \mathcal{Z} is equivalent to the projection onto the closed, convex set $\hat{\mathcal{N}}_{\mathcal{Z}}^*(z^\circ) + \{z^\circ\}$ and therefore enjoys all of the

properties of a projection onto a closed convex set. In particular single-valuedness, continuity and firm non-expansiveness [27, Proposition 4.8, p. 61]. \square

Proof of Claim 1 Given a $\xi > \bar{\xi}$ and local minimum z° to Problem (2), we define the auxiliary set $\mathcal{C}_\xi(z^\circ)$ of fixed points corresponding to z° , where (C.5) is violated

$$\mathcal{C}_\xi(z^\circ) := \{s \in \text{fix } T_\xi|_{z^\circ} \mid s \notin \text{relint } \hat{\mathcal{N}}_{\mathcal{Z}}(z^\circ) + \{z^\circ\}, \text{ or } \mathcal{P}_{\mathcal{Z}}(s) \neq \{z^\circ\}\}.$$

We want to show that for any $\xi > \bar{\xi}$, and any local minimum z° such that $\text{fix } T_\xi|_{z^\circ} \neq \emptyset$, the set $\mathcal{C}_\xi(z^\circ)$ is a measure-zero subset of $\text{fix } T_\xi|_{z^\circ}$. This then implies that (C.5a) and (C.5b) hold for all $s \in \text{fix } T_\xi|_{z^\circ}$ except a measure-zero subset. We consider the two cases:

First, we consider the case where, given a local minimum z° , $\text{fix } T_\xi|_{z^\circ}$ is a singleton set for all $\xi \geq \bar{\xi}$. In particular there exists an s° such that $\{s^\circ\} = \text{fix } T_{\bar{\xi}}|_{z^\circ}$, which by definition implies that $z^\circ \in \mathcal{P}_{\mathcal{Z}}(s^\circ)$. Via [22, Example 6.16, p. 212], this further implies that $\{z^\circ\} = \mathcal{P}_{\mathcal{Z}}(s(\xi))$ for all $\xi > \bar{\xi}$, where $s(\xi) := z^\circ - \frac{1}{\xi} \bar{\xi}(z^\circ - s^\circ)$, and $\{s(\xi)\} = \text{fix } T_\xi|_{z^\circ}$, by definition and Assumption (A2). Furthermore, by Assumption (A2), we have that for all $\xi \geq \bar{\xi}$, it holds that $s(\xi) \in \text{relint } \hat{\mathcal{N}}_{\mathcal{Z}}(z^\circ) + \{z^\circ\}$. Therefore, for all $\xi > \bar{\xi}$, we have that $\mathcal{C}_\xi(z^\circ) = \emptyset$.

Next we consider the case where, given a local minimum z° , $\text{fix } T_\xi|_{z^\circ}$ contains more than one element for all $\xi \geq \bar{\xi}$. We define the sets

$$\begin{aligned} \mathcal{C}_\xi^{\mathcal{N}}(z^\circ) &:= \{s \in \text{fix } T_\xi|_{z^\circ} \mid s \in \text{relbd } \hat{\mathcal{N}}_{\mathcal{Z}}(z^\circ) + \{z^\circ\}\}, \\ \mathcal{C}_\xi^{\mathcal{P}}(z^\circ) &:= \{s \in \text{fix } T_\xi|_{z^\circ} \mid \mathcal{P}_{\mathcal{Z}}(s) \neq \{z^\circ\}\}, \end{aligned}$$

with $\mathcal{C}_\xi(z^\circ) = \mathcal{C}_\xi^{\mathcal{N}}(z^\circ) \cup \mathcal{C}_\xi^{\mathcal{P}}(z^\circ)$. We will show that the sets $\mathcal{C}_\xi^{\mathcal{N}}(z^\circ)$ and $\mathcal{C}_\xi^{\mathcal{P}}(z^\circ)$ are measure-zero subsets of $\text{fix } T_\xi|_{z^\circ}$, which implies that $\mathcal{C}_\xi(z^\circ)$ is a measure-zero subset of $\text{fix } T_\xi|_{z^\circ}$.

We first consider the set $\mathcal{C}_\xi^{\mathcal{N}}(z^\circ)$, which is defined as the union of all the facets of the shifted closed convex polyhedral cone $\hat{\mathcal{N}}_{\mathcal{Z}}(z^\circ) + \{z^\circ\}$ intersected with the convex set $\text{fix } T_\xi|_{z^\circ}$. The cone $\hat{\mathcal{N}}_{\mathcal{Z}}(z^\circ)$ is finitely generated and therefore has a finite number of facets. By Assumption (A2) we know that there exists a $\bar{s} \in \text{fix } T_{\bar{\xi}}|_{z^\circ}$ such that $\bar{s} \in \text{relint } \hat{\mathcal{N}}_{\mathcal{Z}}(z^\circ) + \{z^\circ\}$. Therefore, for each facet \mathcal{F} of $\hat{\mathcal{N}}_{\mathcal{Z}}(z^\circ)$, by convexity of $\text{fix } T_\xi|_{z^\circ}$, we have that $\text{conv}((\mathcal{F} \cap \text{fix } T_\xi|_{z^\circ}) \cup \{\bar{s}\}) \subseteq \text{fix } T_\xi|_{z^\circ}$ and that $\mathcal{F} \cap \text{fix } T_\xi|_{z^\circ}$ is a measure-zero subset of $\text{conv}((\mathcal{F} \cap \text{fix } T_\xi|_{z^\circ}) \cup \{\bar{s}\})$ by virtue of the fact that $\bar{s} \notin \mathcal{F}$. This immediately implies that $\mathcal{F} \cap \text{fix } T_\xi|_{z^\circ}$ is a measure-zero subset of $\text{fix } T_\xi|_{z^\circ}$ and thereby $\mathcal{C}_\xi^{\mathcal{N}}(z^\circ)$ is a measure-zero subset of $\text{fix } T_\xi|_{z^\circ}$.

Now we consider the set $\mathcal{C}_\xi^{\mathcal{P}}(z^\circ)$. Again by convexity of $\text{fix } T_\xi|_{z^\circ}$ we know that the relative boundary

relbd($\text{fix } T_\xi|z^\circ$) of $\text{fix } T_\xi|z^\circ$ is a measure zero subset of $\text{fix } T_\xi|z^\circ$. We will show that $\mathcal{C}_\xi^{\mathcal{P}}(z^\circ) \subseteq \text{relbd}(\text{fix } T_\xi|z^\circ)$. For the sake of arriving at a contradiction, we assume that there exists a $s \in \text{relint}(\text{fix } T_\xi|z^\circ)$ such that there exists a $\bar{z} \neq z^\circ$, with $\{z^\circ, \bar{z}\} \subseteq \mathcal{P}_{\mathcal{Z}}(s)$. By openness and convexity of $\text{relint}(\text{fix } T_\xi|z^\circ)$ there exists a $d \in \mathbb{R}^n$ and $\bar{\epsilon} > 0$, with $\|d\| = 1$ such that $s + \theta d \in \text{fix } T_\xi|z^\circ$ for all $\theta \in [-\bar{\epsilon}, \bar{\epsilon}]$. By definition we have that $z^\circ \in \mathcal{P}_{\mathcal{Z}}(s + \theta d)$ and therefore $\|s + \theta d - z^\circ\| \leq \|s + \theta d - \bar{z}\|$ for all $\theta \in [-\bar{\epsilon}, \bar{\epsilon}]$ and $z \in \mathcal{Z}$. Because $\|s - z^\circ\| = \|s - \bar{z}\|$, we in fact have $0 = \|s - z^\circ\|^2 - \|s - \bar{z}\|^2 \leq \theta \langle z^\circ - \bar{z}, d \rangle$ for all $\theta \in [-\bar{\epsilon}, \bar{\epsilon}]$, a contradiction. Therefore $\mathcal{C}_\xi^{\mathcal{P}}(z^\circ) \subseteq \text{relbd}(\text{fix } T_\xi|z^\circ)$, which implies that the set $\mathcal{C}_\xi^{\mathcal{P}}(z^\circ)$ is also a measure-zero subset of $\text{fix } T_\xi|z^\circ$ and therefore $\mathcal{C}_\xi(z^\circ)$ is a measure-zero subset of $\text{fix } T_\xi|z^\circ$. This means that (C.5) holds for all $s \in \text{fix } T_\xi|z^\circ$ except a measure-zero subset. \square

Proof of Lemma 5 We consider any $\xi > 0$ and $s^\circ \in \text{fix } T_\xi$ such that there exists an $\epsilon > 0$ such that the projection $\mathcal{P}_{\mathcal{Z}}$ is single-valued, continuous and firmly non-expansive on $\mathcal{B}_\epsilon(s^\circ)$. We recall the definition of T_ξ in (11a). Clearly T_ξ is single-valued and continuous on $\mathcal{B}_\epsilon(s^\circ)$ by virtue of the projection. It remains to show the non-expansiveness of T_ξ on $\mathcal{B}_\epsilon(s^\circ)$. By [27, Definition 4.1 (ii), p. 59] T_ξ is non-expansive on $\mathcal{B}_\epsilon(s^\circ)$ if

$$\|T_\xi(s) - T_\xi(t)\|^2 \leq \|s - t\|^2, \quad \forall s, t \in \mathcal{B}_\epsilon(s^\circ).$$

For any s, t , we have by definition of T_ξ , that

$$\begin{aligned} \|T_\xi(s) - T_\xi(t)\|^2 &= \|(I - WM_\xi)(s - t)\|^2 \\ &\quad + 2\langle W^\top(I - WM_\xi)(s - t), \mathcal{P}_{\mathcal{Z}}(s) - \mathcal{P}_{\mathcal{Z}}(t) \rangle \\ &\quad + \|W(\mathcal{P}_{\mathcal{Z}}(s) - \mathcal{P}_{\mathcal{Z}}(t))\|^2. \end{aligned} \quad (\text{C.6})$$

In order to show that (C.6) $\leq \|s - t\|^2$ for all $s, t \in \mathcal{B}_\epsilon(s^\circ)$ we are going to split (C.6) into two parts, the portions belonging to the range- and nullspace of M_ξ . We recall that M_ξ is positive semi-definite for ξ satisfying (9a). Therefore, we can consider the eigenvalue decomposition of M_ξ , as in (11) and define q_i , for $i = 1, \dots, n$, to be the normalized eigenvectors of M_ξ . We define $\delta, p \in \mathbb{R}^n$ as the coefficients of linear combinations of the eigenvectors of M_ξ , such that $\sum_{i=1}^n \delta_i q_i = s - t$ and $\sum_{i=1}^n p_i q_i = \mathcal{P}_{\mathcal{Z}}(s) - \mathcal{P}_{\mathcal{Z}}(t)$. We further define $\delta^\perp := \sum_{i=1}^{n-m} \delta_i q_i$, $\delta^0 := \sum_{i=n-m+1}^n \delta_i q_i$, $p^\perp := \sum_{i=1}^{n-m} p_i q_i$ and $p^0 := \sum_{i=n-m+1}^n p_i q_i$, which splits $s - t$ and $\mathcal{P}_{\mathcal{Z}}(s) - \mathcal{P}_{\mathcal{Z}}(t)$ into their range and nullspace portions. Substituting $\delta^\perp, \delta^0, p^\perp$ and p^0 into (C.6), using the eigenvalue decomposition of M_ξ and W as defined in (11b), we obtain

$$\begin{aligned} \|T_\xi(s) - T_\xi(t)\|^2 &= \frac{1}{4}\|\delta^\perp\|^2 + \|\delta^0\|^2 \\ &\quad + \frac{1}{2}\langle \delta^\perp, p_\Lambda^\perp \rangle - 2\langle \delta^0, p^0 \rangle \\ &\quad + \frac{1}{4}\|p_\Lambda^\perp\|^2 + \|p^0\|^2, \end{aligned} \quad (\text{C.7})$$

where $p_\Lambda^\perp := \sum_{i=1}^{n-m} \lambda_i^{-1} p_i q_i$ for λ_i the non-zero eigenvalues of M_ξ . We want to show that (C.7) $\leq \|s - t\|^2 = \|\delta^\perp\|^2 + \|\delta^0\|^2$. However, this only has to hold for δ, p that are related via the projection $\mathcal{P}_{\mathcal{Z}}$ where in particular we want to exploit its firm non-expansiveness. The projection $\mathcal{P}_{\mathcal{Z}}$ being firmly non-expansive on $\mathcal{B}_\epsilon(s^\circ)$, means by [27, Proposition 4.2 (iv), p. 60], that for all $s, t \in \mathcal{B}_\epsilon(s^\circ)$

$$\|\mathcal{P}_{\mathcal{Z}}(s) - \mathcal{P}_{\mathcal{Z}}(t)\|^2 \leq \langle s - t, \mathcal{P}_{\mathcal{Z}}(s) - \mathcal{P}_{\mathcal{Z}}(t) \rangle. \quad (\text{FNE})$$

It is also non-expansive, i.e., for any $s, t \in \mathcal{B}_\epsilon(s^\circ)$

$$\|\mathcal{P}_{\mathcal{Z}}(s) - \mathcal{P}_{\mathcal{Z}}(t)\|^2 \leq \|s - t\|^2, \quad (\text{NE})$$

By applying the Cauchy-Schwarz inequality, and combining (FNE) and (NE) we finally get

$$\begin{aligned} 0 &\leq \|\mathcal{P}_{\mathcal{Z}}(s) - \mathcal{P}_{\mathcal{Z}}(t)\|^2 \\ &\leq \langle s - t, \mathcal{P}_{\mathcal{Z}}(s) - \mathcal{P}_{\mathcal{Z}}(t) \rangle \leq \|s - t\|^2. \end{aligned} \quad (\text{C.8})$$

We can also substitute $\delta^\perp, \delta^0, p^\perp$ and p^0 into (C.8) obtaining

$$\begin{aligned} 0 &\leq \|p^\perp\|^2 + \|p^0\|^2 \\ &\leq \langle p^\perp, \delta^\perp \rangle + \langle p^0, \delta^0 \rangle \leq \|\delta^\perp\|^2 + \|\delta^0\|^2. \end{aligned} \quad (\text{C.9})$$

To show that T_ξ is non-expansive it is therefore sufficient to show that for all δ, p that satisfy (C.9) it holds that (C.7) $\leq \|\delta^\perp\|^2 + \|\delta^0\|^2$. Notice, that (C.7) and (C.9) do not contain any coupling terms between range- and nullspace portions of δ or p , therefore we can argue about them separately.

i) We want to show that for all δ^\perp, p^\perp such that

$$0 \leq \|p^\perp\|^2 \leq \langle p^\perp, \delta^\perp \rangle \leq \|\delta^\perp\|^2, \quad (\text{C.10})$$

we have that

$$\frac{1}{4}\|\delta^\perp\|^2 + \frac{1}{2}\langle \delta^\perp, p_\Lambda^\perp \rangle + \frac{1}{4}\|p_\Lambda^\perp\|^2 \leq \|\delta^\perp\|^2.$$

Given p^\perp, δ^\perp such that (C.10) holds, using (9b) implies that $\|\Lambda^{-1}\|_2 \leq 1$ thus we obtain $\|p_\Lambda^\perp\| \leq \|p^\perp\| \leq \|\delta^\perp\|$ and $\langle \delta^\perp, p_\Lambda^\perp \rangle \leq \|\delta^\perp\|^2$. Therefore

$$\begin{aligned} &\frac{1}{4}\|\delta^\perp\|^2 + \frac{1}{2}\langle \delta^\perp, p_\Lambda^\perp \rangle + \frac{1}{4}\|p_\Lambda^\perp\|^2 \\ &\leq \frac{1}{4}\|\delta^\perp\|^2 + \frac{1}{2}\|\delta^\perp\|^2 + \frac{1}{4}\|\delta^\perp\|^2 = \|\delta^\perp\|^2. \end{aligned}$$

ii) We want to show that for all δ^0, p^0 such that

$$0 \leq \|p^0\|^2 \leq \langle p^0, \delta^0 \rangle \leq \|\delta^0\|^2,$$

we have that

$$\|\delta^0\|^2 - 2\langle \delta^0, p^0 \rangle + \|p^0\|^2 \leq \|\delta^0\|^2.$$

We consider

$$\begin{aligned} & \|\delta^0\|^2 - 2\langle \delta^0, p^0 \rangle + \|p^0\|^2 \\ & \leq \|\delta^0\|^2 - 2\langle \delta^0, p^0 \rangle + \langle \delta^0, p^0 \rangle \leq \|\delta^0\|^2. \end{aligned}$$

Cases i) and ii) together imply the result. \square

D Algorithm for checking (A3)

In this section, we give an algorithm for checking Assumption (A3). The assumption is purely geometrical and needs to be satisfied at every point in \mathcal{Z} . Therefore the algorithm will effectively enumerate all possible combinations of active components and their active sets and check for each such combination. This amounts to a finite (but combinatorial) number of checks. Note that checking a parametric set $\mathcal{Z}(\theta)$, due to the polyhedral structure, amounts to checking finitely many different non-parametric sets. Therefore $\mathcal{Z}(\theta)$ can be checked once and “offline” for all θ .

We begin by defining the *active set* $\mathcal{J}_{\mathcal{Z}(\theta)}(z)$ of $\mathcal{Z}(\theta)$, with parameter $\theta \in \mathbb{R}^p$, at $z \in \mathcal{Z}$, as the collection of all the active sets of the components of $\mathcal{Z}(\theta)$, i.e., $\mathcal{J}_{\mathcal{Z}(\theta)}(z) := \{\mathcal{J}_{\mathcal{Z}^i(\theta)}(z)\}_{i=1}^I$, where the active set $\mathcal{J}_{\mathcal{Z}^i(\theta)}(z)$ of a polyhedron $\mathcal{Z}^i(\theta)$ is defined in the usual way [19, Definition 12.1, p. 308] as the set of constraints active at $z \in \mathcal{Z}^i(\theta)$ and $\mathcal{J}_{\mathcal{Z}^i(\theta)}(z) = \emptyset$ if $z \notin \mathcal{Z}^i(\theta)$. The set $\mathcal{I}_{\mathcal{Z}} \subseteq 2^{\{1, \dots, I\}}$ denotes the set of sets of active components of $\mathcal{Z}(\theta)$, i.e., $\mathcal{I} \in \mathcal{I}_{\mathcal{Z}(\theta)}$ if and only if there exists θ and $z \in \mathcal{Z}(\theta)$ such that $\mathcal{I} \equiv \mathcal{I}_{\mathcal{Z}(\theta)}(z)$. Similarly we denote by $\mathcal{J}_{\mathcal{Z}(\theta)}$ the set of all possible active sets of $\mathcal{Z}(\theta)$

$$\mathcal{J}_{\mathcal{Z}(\theta)} := \left\{ \left\{ \mathcal{J}_i \right\}_{i=1}^I \mid \exists \theta \in \mathbb{R}^p, \exists z \in \mathcal{Z}(\theta) \text{ s. t. } \left\{ \mathcal{J}_i \right\}_{i=1}^I \equiv \mathcal{J}_{\mathcal{Z}(\theta)}(z) \right\},$$

We will consider $\mathcal{Z}(\theta)$ with components $\mathcal{Z}^i(\theta)$ defined as

$$\mathcal{Z}(\theta) = \bigcup_{i=1}^I \underbrace{\{z \mid F^i z \leq f^i(\theta), G^i z = g^i(\theta)\}}_{\mathcal{Z}^i(\theta)}, \quad (\text{D.1})$$

where $F^i \in \mathbb{R}^{m_i \times n}$, $G^i \in \mathbb{R}^{p_i \times n}$ and $f^i \in \mathbb{R}^{m_i}$. The functions $f^i(\theta) = F^{i,\theta} + f^i$ and $g^i(\theta) = G^{i,\theta} + g^i$ depend affinely on a parameter $\theta \in \mathbb{R}^p$. With $\mathcal{Z}^i(\theta)$ closed convex polyhedra for fixed θ and non-empty for some θ . Given a component i and one of its active sets \mathcal{J}_i , then $F_{\mathcal{J}_i}^i$ denotes the subset of rows of F^i that belong to the active set \mathcal{J}_i , $f_{\mathcal{J}_i}^i$ is defined in the same way.

Lemma D.1 *Given a (parametric) set $\mathcal{Z}(\theta)$ as in (D.1), then Algorithm 3 terminates in a finite number of steps. Either $\mathcal{Z}(\theta)$ satisfies Assumption (A3) for all θ , or the algorithm returns a valid counter-example.*

Algorithm 3 Check of Assumption (A3)

Require: $\mathcal{Z}(\theta)$ as in (D.1)

```

1: for each  $\mathcal{I} \in \mathcal{I}_{\mathcal{Z}(\theta)}$ ,  $\{\mathcal{J}_i\}_{i=1}^I \in \mathcal{J}_{\mathcal{Z}(\theta)}$  do
2:    $\mathcal{N} \leftarrow \bigcap_{i \in \mathcal{I}} \{v \mid v = (F_{\mathcal{J}_i}^i)^\top \mu + (G^i)^\top \nu, \mu \geq 0\}$ 
3:   if  $\mathcal{N} = \{0\}$  then
4:     continue
5:   for each  $i \in \mathcal{I}$  do
6:      $\mathcal{R}_i = \{v \mid F_{\mathcal{J}_i}^i v \leq 0, G^i v = 0\}$ 
7:    $\mathcal{R} \leftarrow \bigcup_{i \in \mathcal{I}} \mathcal{R}_i$ 
8:   if  $\mathcal{N}^\perp \subseteq \mathcal{R}$  then
9:     continue
10:  else
11:     $w \leftarrow w \in \mathcal{N}^\perp \setminus \mathcal{R}$ 
12:    return  $(w, \{\mathcal{A}_j\}_{j=1}^m)$   $\triangleright$  Counter-example
```

Algorithm 3 is a combinatorial algorithm and may perform badly for anything but small dimensions. However, since by assumption the set \mathcal{Z} is a Cartesian product of sets in low dimension, the check can be performed separately for each part of the Cartesian product. This significantly reduces the “curse of dimensionality”.

Proof of Lemma D.1 We will show that Algorithm 3 effectively checks Assumption (A3) for every θ and every point in $\mathcal{Z}(\theta)$. We will argue, that checking (A3) for every $\theta \in \mathbb{R}^p$ and every $z \in \mathcal{Z}(\theta)$ is equivalent to checking it for every set of active constraints. Note that $\mathcal{A}_{\mathcal{Z}(\theta)}$ the set of active sets of $\mathcal{Z}(\theta)$ is a finite set with at most $2^{\bar{m}}$ elements, where $\bar{m} := \sum_{i=1}^I m_i$. We further note that $\mathcal{I}_{\mathcal{Z}(\theta)}$ and $\mathcal{J}_{\mathcal{Z}(\theta)}$ can be constructed by solving a finite number of linear programs.

In Algorithm 3, we iterate over the elements of $\mathcal{I}_{\mathcal{Z}(\theta)}$ and $\mathcal{J}_{\mathcal{Z}(\theta)}$, which means that the loop is executed at most a finite number of times. For each pair $\mathcal{I}, \{\mathcal{J}_i\}_{i=1}^I$ we want to verify, or invalidate, (A3) by looking at two sets \mathcal{N} and \mathcal{R} , these set are defined solely via the active constraints and do not depend on θ , since θ only affects the sets $\mathcal{I}_{\mathcal{Z}(\theta)}$ and $\mathcal{J}_{\mathcal{Z}(\theta)}$. Given a pair $\mathcal{I}, \{\mathcal{J}_i\}_{i=1}^I$, for each active component $i \in \mathcal{I}$ we can define two auxiliary sets

$$\begin{aligned} \mathcal{A}_i(\theta) &:= \{z \mid F_{\mathcal{J}_i}^i z = f_{\mathcal{J}_i}^i(\theta), F_{\mathcal{J}_i^c}^i z < f_{\mathcal{J}_i^c}^i(\theta), \\ & \quad G^i z = g^i(\theta)\}, \\ \mathcal{F}_i(\theta) &:= \{z \mid F_{\mathcal{J}_i}^i z \leq f_{\mathcal{J}_i}^i(\theta), G^i z = g^i(\theta)\}, \end{aligned}$$

where the set \mathcal{J}_i^c is simply the complement of \mathcal{J}_i , i.e., the set of constraints that are not active. For a given θ , set $\mathcal{A}_i(\theta)$ is the set of points $z \in \mathcal{Z}$ that belong to the active set \mathcal{J}_i , whereas $\mathcal{F}_i(\theta) \supseteq \mathcal{A}_i(\theta)$ is a larger set, that is defined by only the active constraints and in general is not included in \mathcal{Z} . For a pair $\mathcal{I}, \{\mathcal{J}_i\}_{i=1}^I$ we can further define $\mathcal{A}(\theta) := \bigcap_{i=1}^I \mathcal{A}_i(\theta)$, the set of points that belong to all of the active sets of the active components. By checking Assumption (A3) for each $\mathcal{A}(\theta)$ we will effectively check it for each $z \in \mathcal{Z}$.

The conditions to be checked involve the regular normal cone $\hat{\mathcal{N}}_{\mathcal{Z}(\theta)}(z)$. For each θ , $z \in \mathcal{A}(\theta)$ we can fully characterize the regular normal cone $\hat{\mathcal{N}}_{\mathcal{Z}(\theta)}(z)$, using Proposition C.1 and [22, Theorem 6.46, p. 231]

$$\hat{\mathcal{N}}_{\mathcal{Z}(\theta)}(z) = \bigcap_{i \in \mathcal{I}} \{(F_{\mathcal{F}_i}^i)^\top \mu + (G^i)^\top \nu \mid \mu \geq 0\}.$$

We see that $\hat{\mathcal{N}}_{\mathcal{Z}(\theta)}(z)$ is independent of θ and z , it only depends on which constraints (and components) are active. This set, $\mathcal{N} := \hat{\mathcal{N}}_{\mathcal{Z}(\theta)}(z)$, is computed in step 2 of Algorithm 3. A half-space representation of \mathcal{N} can be obtained using Fourier-Motzkin elimination [32, p. 84] for each i , after which the intersections are trivial. We now need to check two conditions. If \mathcal{N} is equivalent to $\{0\}$, then the first part of (A3) is satisfied for all $z \in \mathcal{A}(\theta)$, and we continue with the next active set. Otherwise we need to check whether there exists an $\epsilon > 0$ such that for all $w \in \mathcal{N}^\perp \cap \mathcal{B}_\epsilon$ we have that $z+w \in \mathcal{Z}(\theta)$. In order to check this condition, in steps 6–7, we construct the set \mathcal{R} as the union of the recession cones $\mathcal{R}_i := \text{rec}(\mathcal{F}_i(\theta))$ of $\mathcal{F}_i(\theta)$. Finally it remains to show

that checking this condition for all $z \in \mathcal{A}(\theta)$, in step 8, is equivalent to checking whether the orthogonal complement $\mathcal{N}^\perp := \{v \in \mathbb{R}^n \mid \langle v, u \rangle = 0, \forall u \in \mathcal{N}\}$ is contained in \mathcal{R} . If $\mathcal{N}^\perp \subseteq \mathcal{R}$, consider any $z \in \mathcal{A}(\theta)$, an $\epsilon > 0$ small enough and any $w \in \mathcal{N}^\perp \cap \mathcal{B}_\epsilon$. Clearly there exists an $i \in \mathcal{I}$ such that $w \in \mathcal{R}_i$. Furthermore, by construction of $\mathcal{A}(\theta)$ and \mathcal{R}_i , we have $z+w \in \mathcal{Z}^i \subseteq \mathcal{Z}$, which can be verified simply by checking that the constraints of \mathcal{Z}^i are not violated.

If \mathcal{R} does not contain \mathcal{N}^\perp , then there exists a $w \in \mathcal{N}^\perp$ such that $w \notin \mathcal{R}_i$, for all $i \in \mathcal{I}$. Because \mathcal{N} and \mathcal{R}_i are cones, this is true for all positive scalings of w . In particular, for any $\epsilon > 0$ there exists a $\nu > 0$ such that $\nu w \in \mathcal{N}^\perp \cap \mathcal{B}_\epsilon$ and $\nu w \notin \mathcal{R}$. Analogously to above, it follows that for any $z \in \mathcal{A}(\theta)$, $z + \nu w \notin \mathcal{Z}^i$ for all $i \in \mathcal{I}$, and therefore $z + \nu w \notin \mathcal{Z}$, which violates (A3). Then, the algorithm terminates and returns a violating direction w and the corresponding active set, from which violating z, θ can be reconstructed. Because the Algorithm 3 enumerates all active sets, it either terminates with a counterexample, or it returns after finitely many steps, having checked all possibilities. \square